



The Abdus Salam  
International Centre for Theoretical Physics



2048-17

**From Core to Crust: Towards an Integrated Vision of Earth's Interior**

*20 - 24 July 2009*

**Towards self consistent models of plate tectonics**

S. Sobolev

*Geoforschungszentrum Potsdam, Germany*

# Towards internally consistent models of plate tectonics

Stephan Sobolev  
and  
Geodynamic Modeling Section

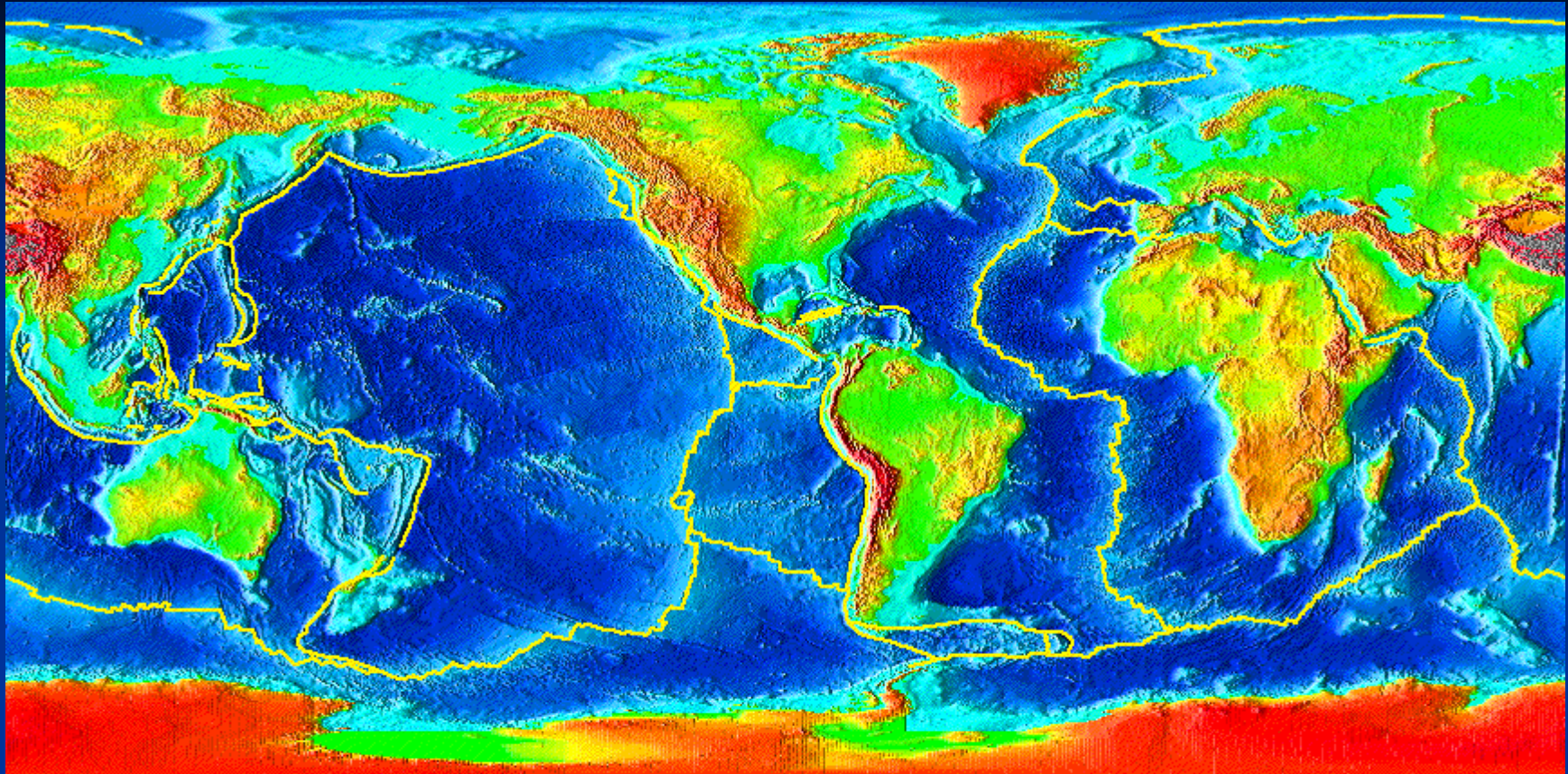


German Research Centre for Geosciences

# Outline

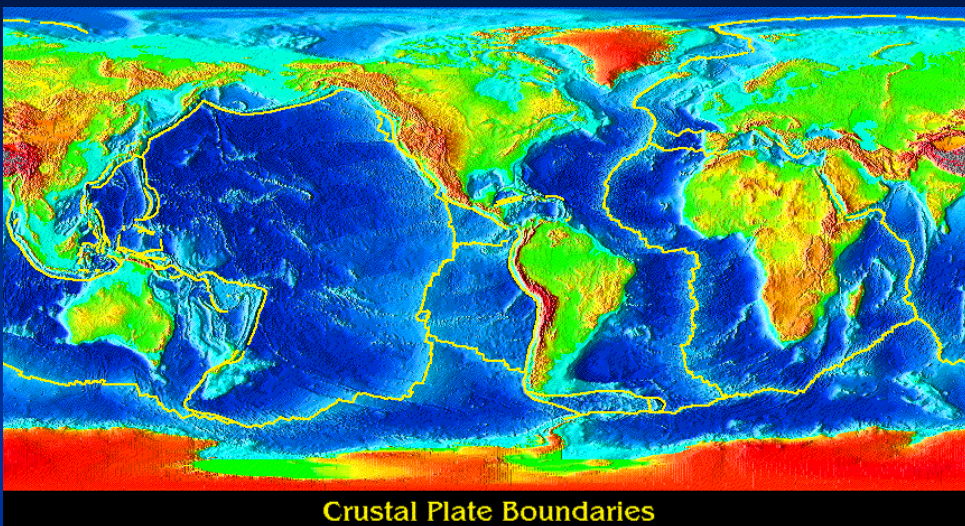
- Ingredients of plate tectonics
- Tools to model 3D deformation at plate boundaries
- Regional scale: Modeling birth and maturation of the plate boundary – *Dead Sea Transform in the Middle East*
- Global scale: Linking mantle convection and lithospheric deformations
  - *How weak are the plate boundaries?*
  - *How weak is asthenosphere?*
  - *Making plate boundaries*

# Plates

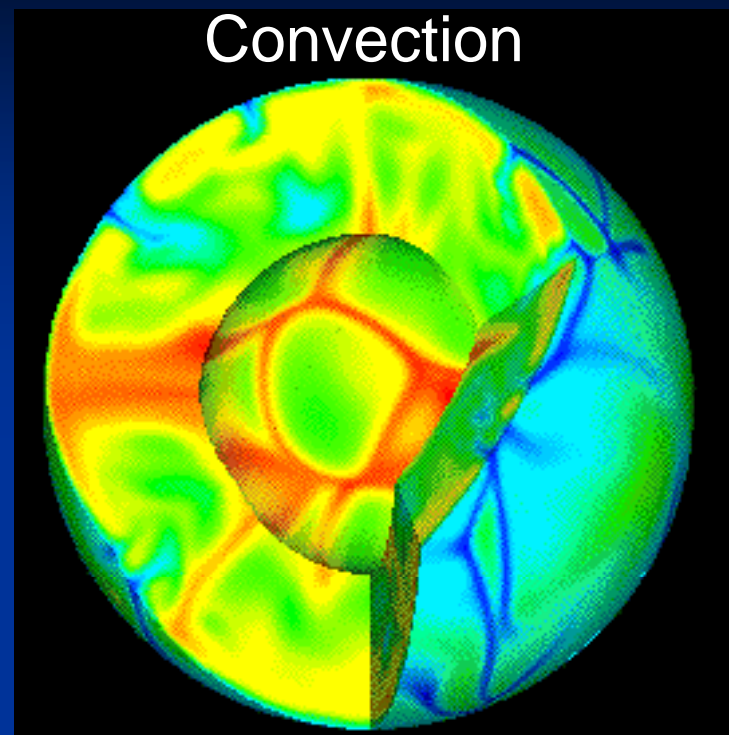


**Earth is a plate-tectonics planet, where most of deformation at the lithospheric level goes at the plate boundaries.**

# Ingredients of plate tectonics



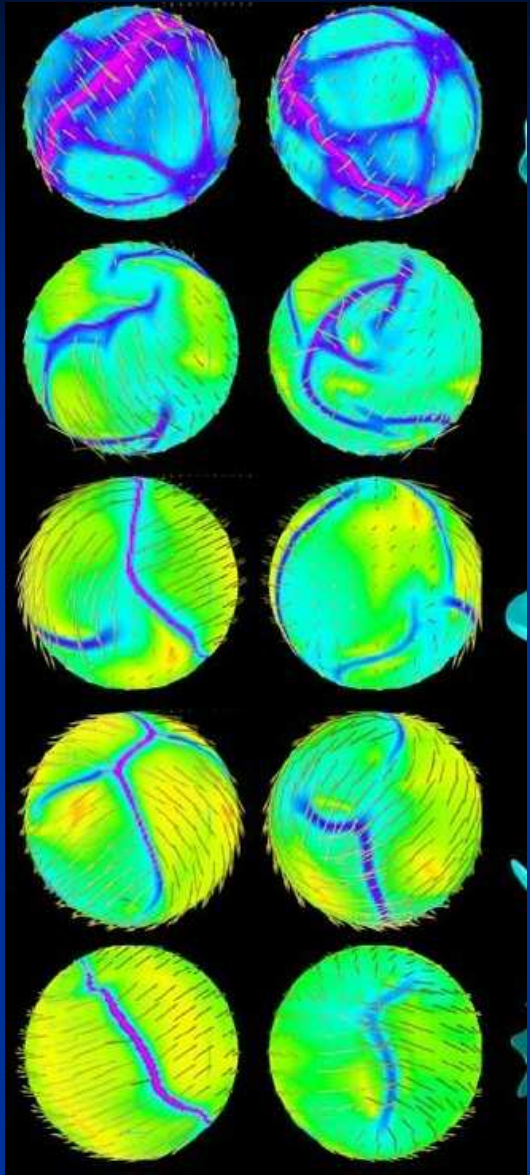
Weak plate boundaries



Ricard and Vigny, 1989; Bercovici, 1993, Bird, 1998; Moresi and Solomatov, 1998; Tackley, 1998, Zhong et al, 1998; Gurnis et al., 2000....

# Ingredients of plate tectonics

Increasing yield stress



Generating plate boundaries

Bercovici, 1993, 1995, 1996,  
1998, 2003; Tackley, 1998,  
2000; Moresi and Solomatov,  
1998; Zhong et al, 1998; Gurnis  
et al., 2000...

**Tendency: towards more realistic  
strongly non-linear rheology**

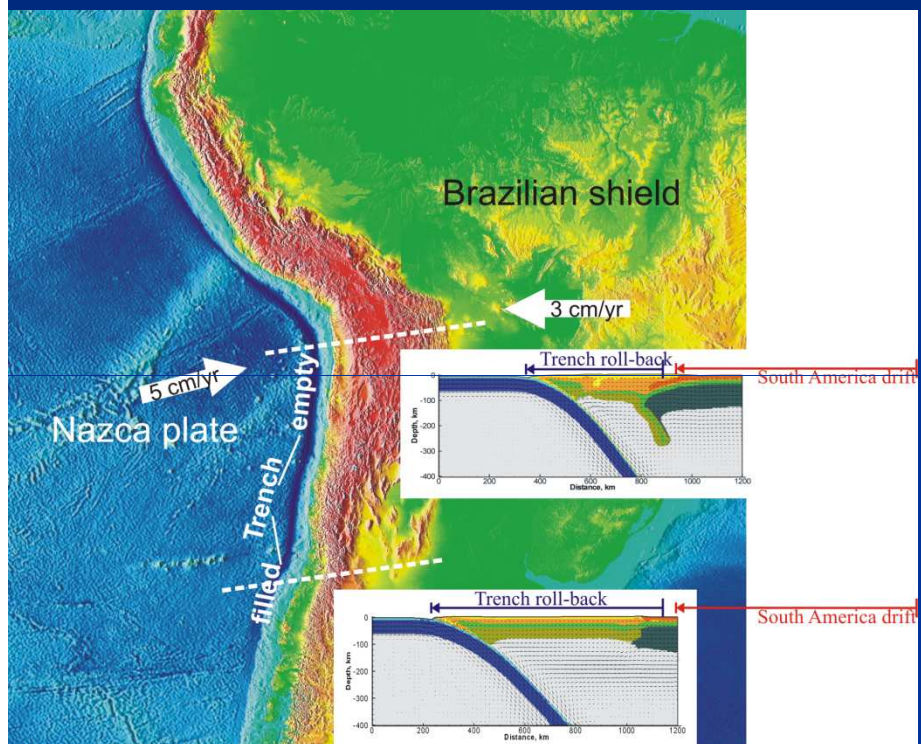
**Viscous rheology-only and  
emulation of brittle failure**

van Heck and Tackley, 2008

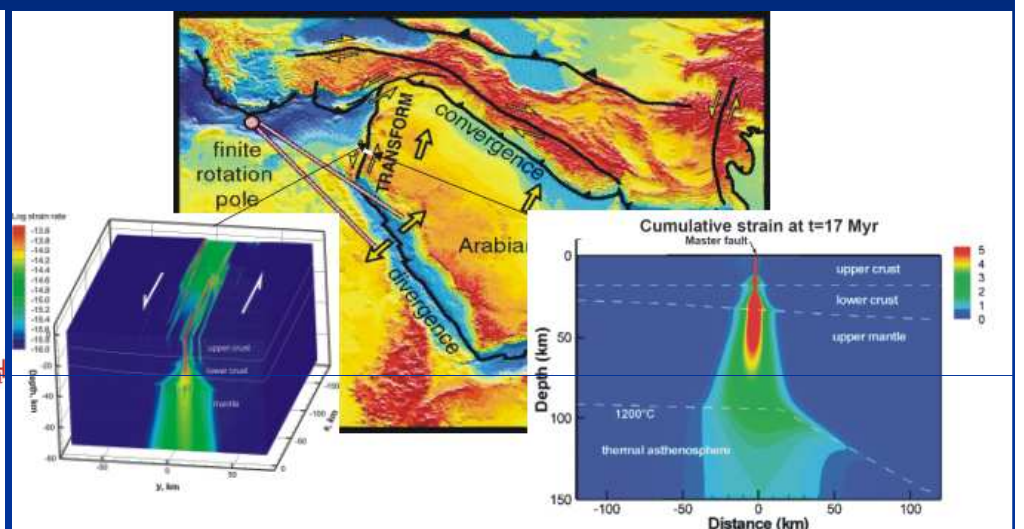
The present-day global models can not reproduce realistic one-sided subduction and pure transform boundaries

# Modeling deformation at plate boundaries

## Subduction and orogeny in Andes



## Dead Sea Transform



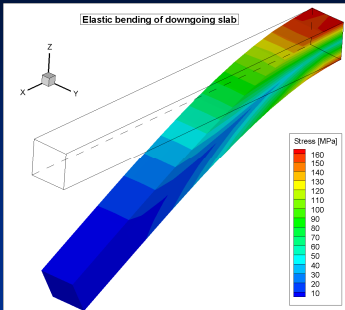
(Sobolev et al., *EPSL* 2005, Petrunin and Sobolev, *Geology* 2006, PEPI, 2008).

Babeyko and Sobolev, *Geology* 2005, Sobolev and Babeyko, *Geology* 2005; Sobolev et al., 2006

# Balance equations „Realistic“ rheology

Momentum:  $\frac{\partial \sigma_{ij}}{\partial x_j} + \Delta \rho g z_i = 0$

Energy:  $\frac{DU}{Dt} = -\frac{\partial q_i}{\partial x_i} + r$



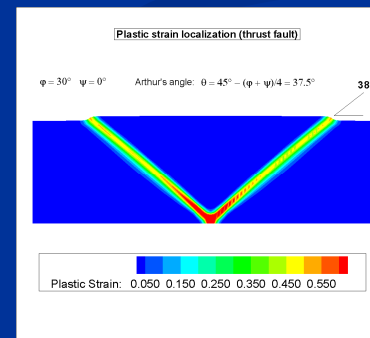
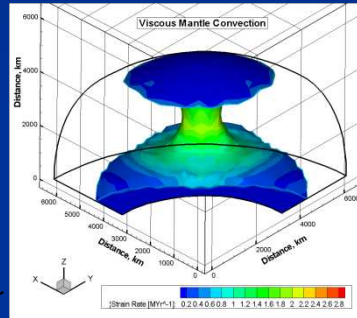
## Deformation mechanisms

$$\dot{\varepsilon}_{ij} = \dot{\varepsilon}_{ij}^{el} + \dot{\varepsilon}_{ij}^{vs} + \dot{\varepsilon}_{ij}^{pl}$$

Elastic strain:  $\dot{\varepsilon}_{ij}^{el} = \frac{1}{2G} \hat{\tau}_{ij}$

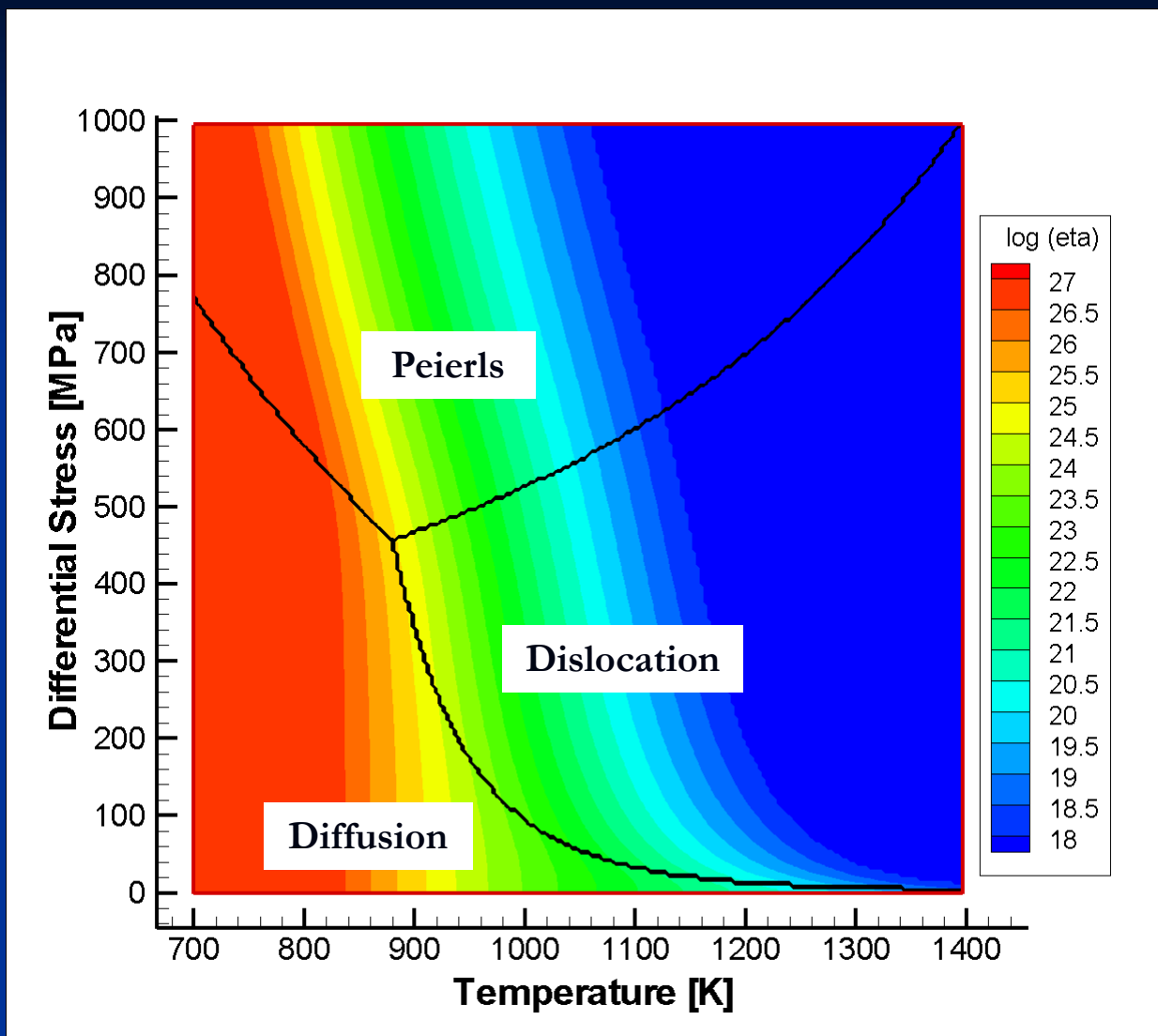
Viscous strain:  $\dot{\varepsilon}_{ij}^{vs} = \frac{1}{2\eta_{eff}} \tau_{ij}$

Plastic strain:  $\dot{\varepsilon}_{ij}^{pl} = \dot{\gamma} \frac{\partial Q}{\partial \tau_{ij}}$   
Mohr-Coulomb



Popov and Sobolev ( PEPI, 2008)

# Three creep processes



$$\eta_{\text{eff}} = \frac{1}{2} \tau_H \left( \dot{\varepsilon}_L + \dot{\varepsilon}_N + \dot{\varepsilon}_P \right)^{-1}$$

Diffusion creep

$$\dot{\varepsilon}_L = B_L \tau_H \exp\left(-\frac{E_L}{RT}\right)$$

Dislocation creep

$$\dot{\varepsilon}_N = B_N \left(\tau_H\right)^n \exp\left(-\frac{E_N}{RT}\right)$$

Peierls creep

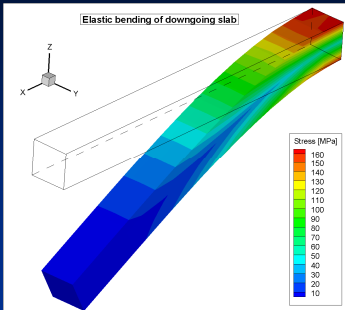
$$\dot{\varepsilon}_P = B_P \exp\left[-\frac{E_P}{RT} \left(1 - \frac{\tau_H}{\tau_P}\right)^2\right]$$

( Kameyama *et al.* 1999)

# Balance equations „Realistic“ rheology

Momentum:  $\frac{\partial \sigma_{ij}}{\partial x_j} + \Delta \rho g z_i = 0$

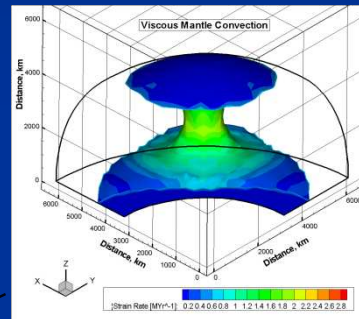
Energy:  $\frac{DU}{Dt} = -\frac{\partial q_i}{\partial x_i} + r$



## Deformation mechanisms

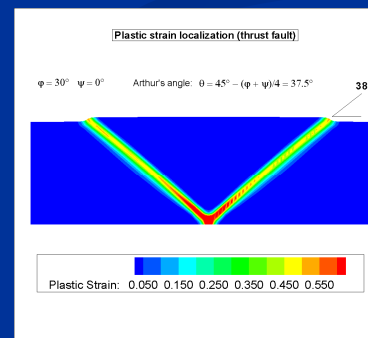
$$\dot{\epsilon}_{ij} = \dot{\epsilon}_{ij}^{el} + \dot{\epsilon}_{ij}^{vs} + \dot{\epsilon}_{ij}^{pl}$$

Elastic strain:  $\dot{\epsilon}_{ij}^{el} = \frac{1}{2G} \hat{\tau}_{ij}$



Viscous strain:  $\dot{\epsilon}_{ij}^{vs} = \frac{1}{2\eta_{eff}} \tau_{ij}$

Plastic strain:  $\dot{\epsilon}_{ij}^{pl} = \dot{\gamma} \frac{\partial Q}{\partial \tau_{ii}}$



Popov and Sobolev ( PEPI, 2008)

# Plasticity

## Mohr-Coulomb plasticity

$$\tau \leq Y = c + \mu_e \cdot \sigma_n$$

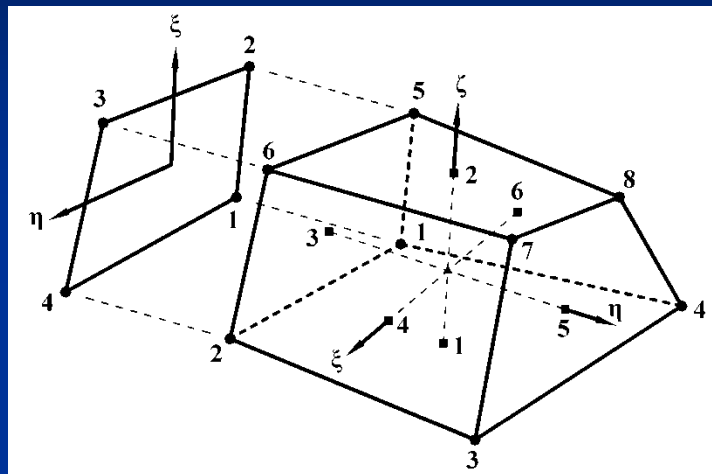
## Damage rheology: strain softening

$$\mu_e = \max(\mu_e^0(1 - a \cdot \xi), \mu_e^1)$$

$$\frac{d\xi}{dt} = \dot{\gamma} - \xi / \tau \quad \mu_e^0 = 0.3 - 0.8$$

# Numerical background

Discretization by  
Finite Element Method



Fast implicit time stepping  
+ Newton-Raphson solver

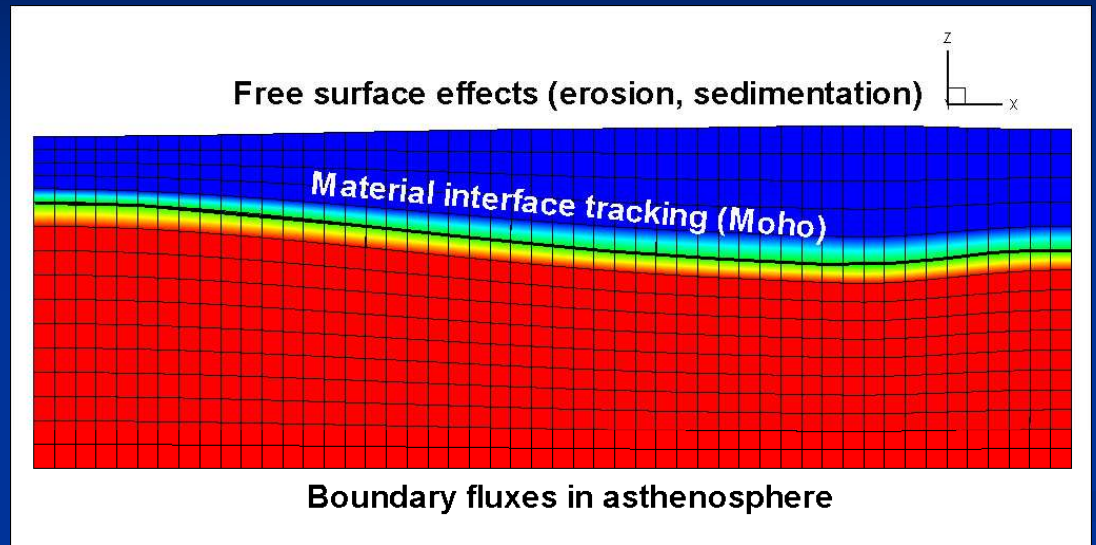
$$\mathbf{u}_{k+1} = \mathbf{u}_k - \mathbf{K}_k^{-1} \mathbf{r}_k$$

$\mathbf{r}$  – Residual Vector

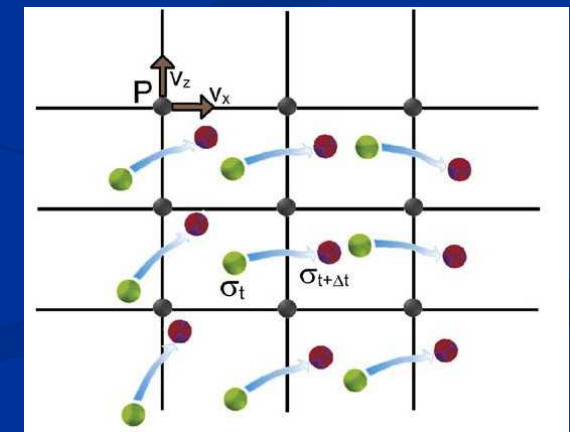
$$\mathbf{K} = \frac{\partial \mathbf{r}}{\partial \Delta \mathbf{u}} \quad \text{Tangent Matrix}$$

Popov and Sobolev (PEPI 2008)

Arbitrary Lagrangian-Eulerian  
kinematical formulation with  
free surface

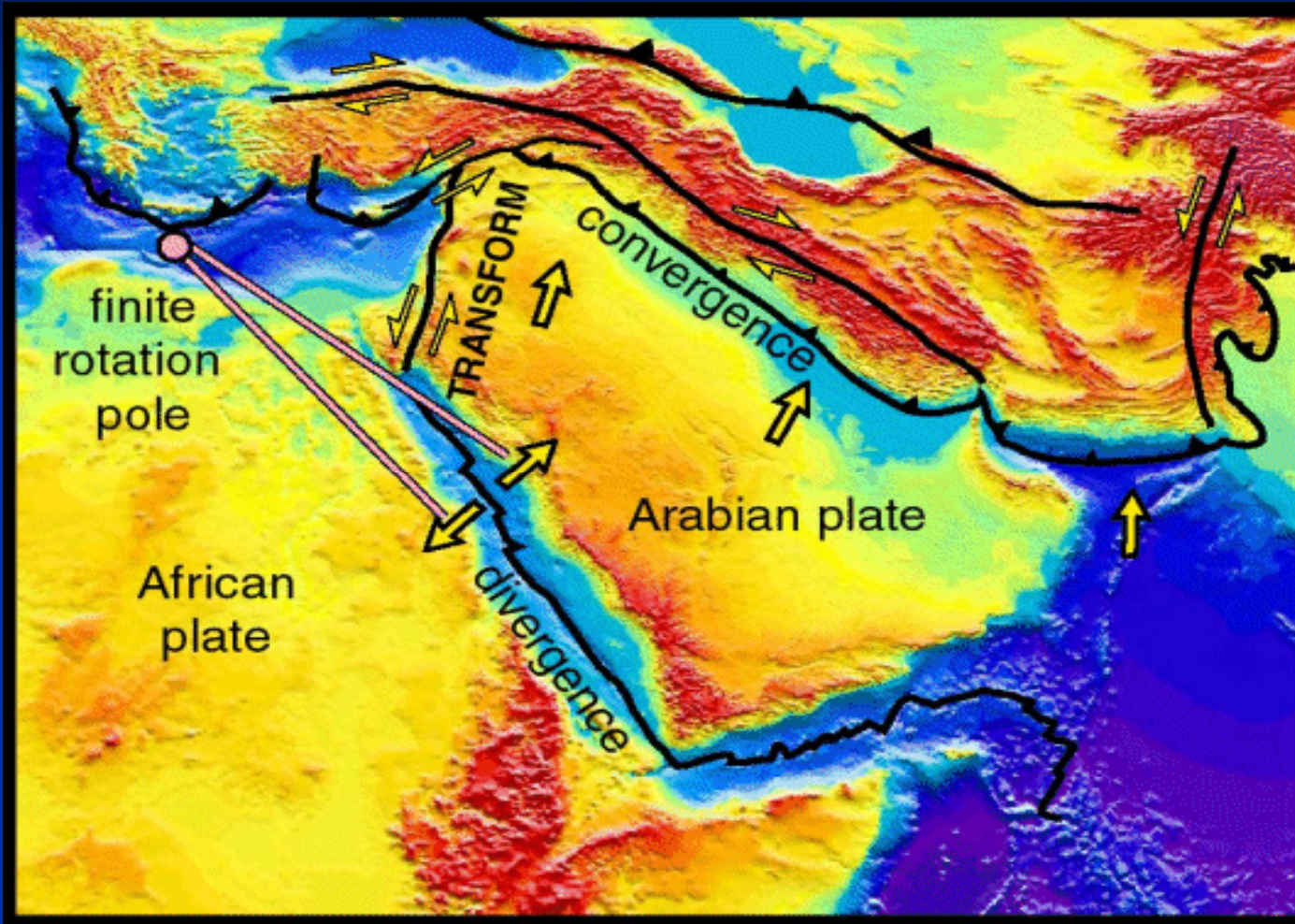


Remapping of  
entire fields by  
Particle-In-Cell  
technique



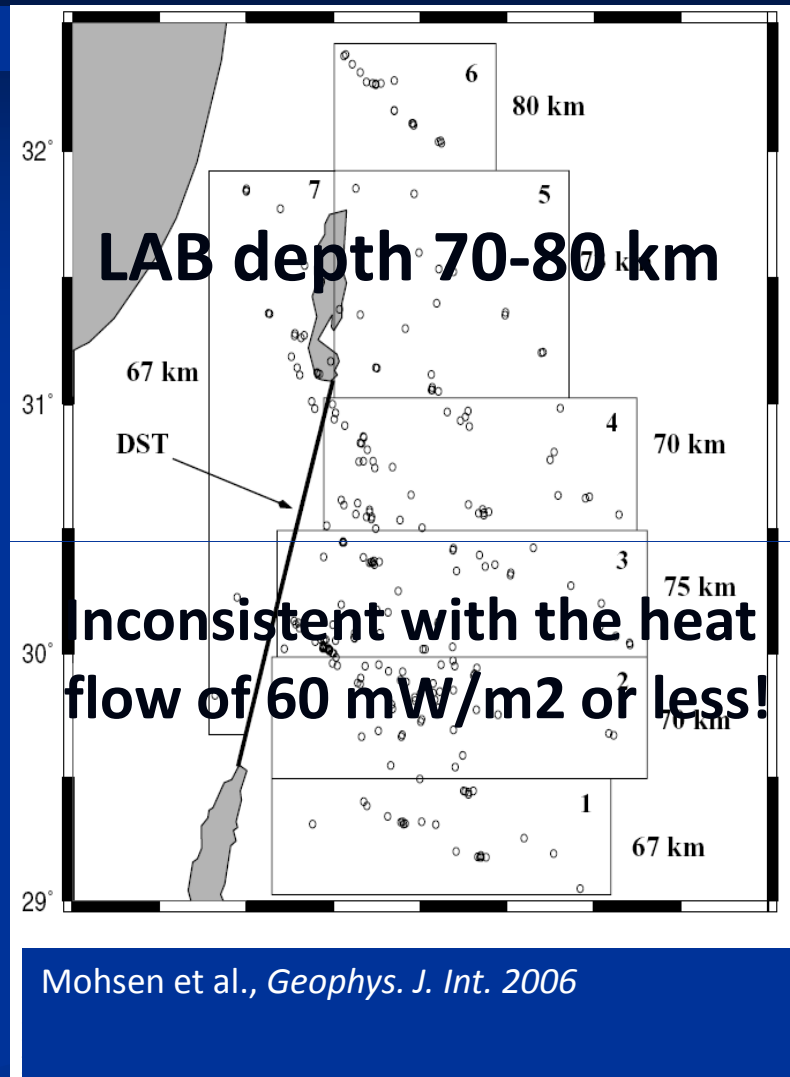
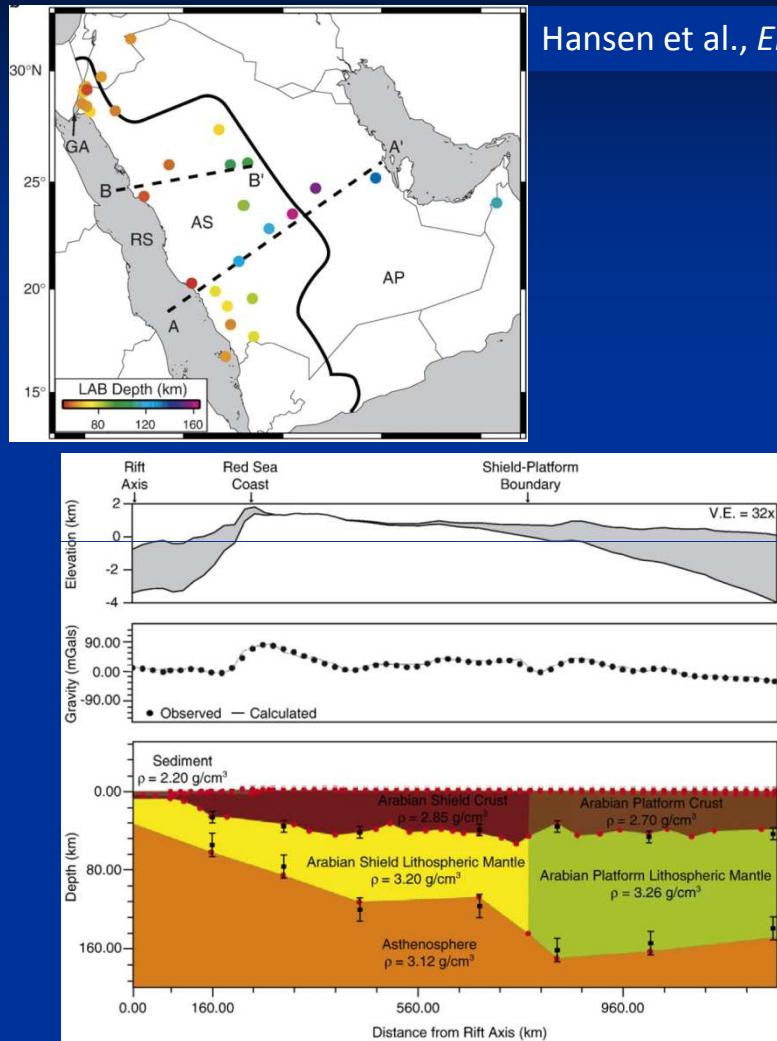
# Transform Fault- case Dead Sea Transform

(In cooperation with A. Petrunin)



How Dead Sea Transform has been formed?

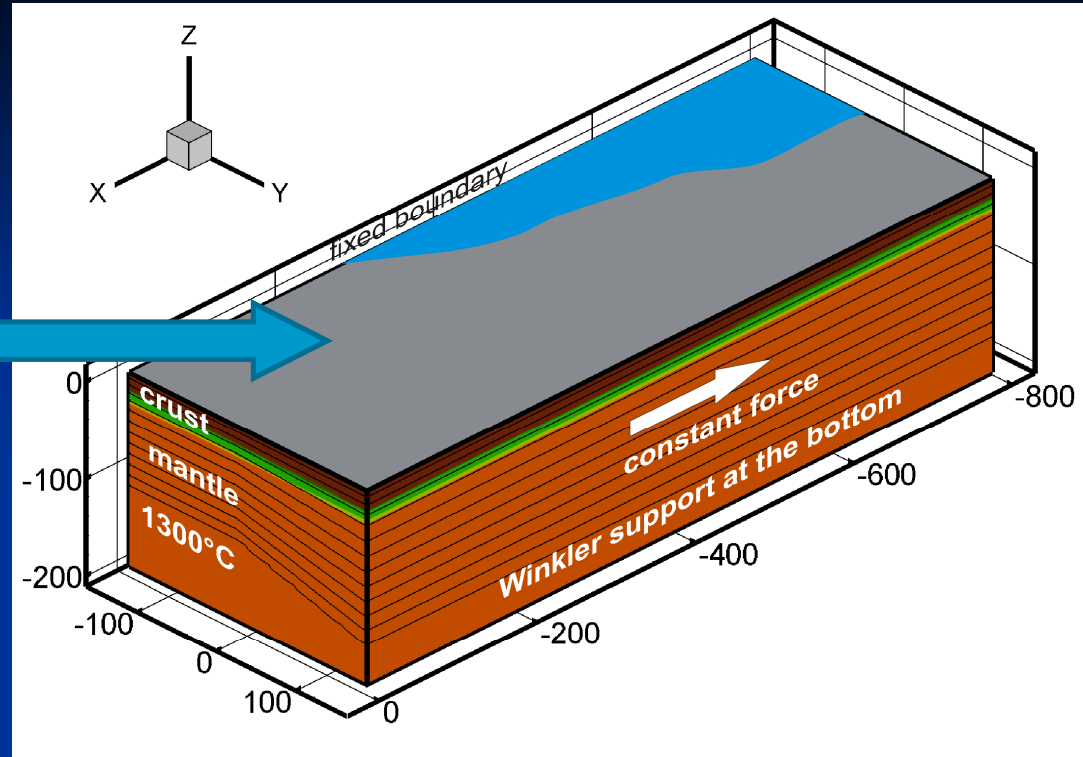
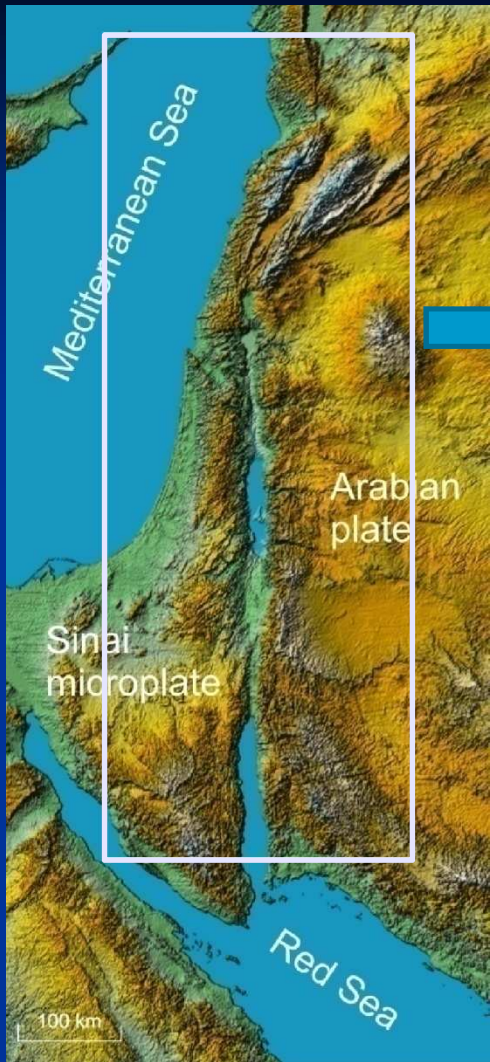
# Present day lithospheric thickness



# Conclusion

Lithosphere around DST was thinned in the past (between 25-15 Ma), such that related high heat flow had not enough time to reach the surface

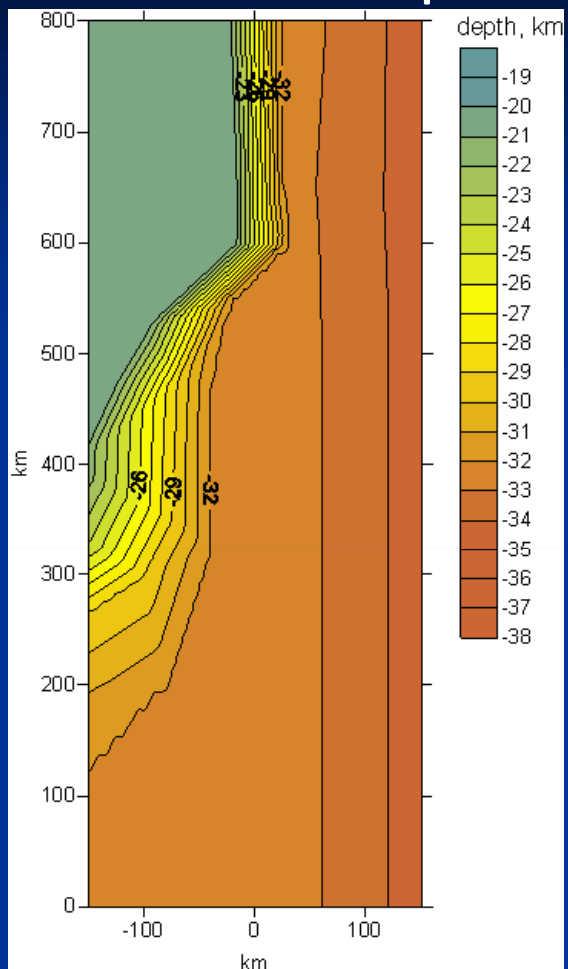
# Model setup



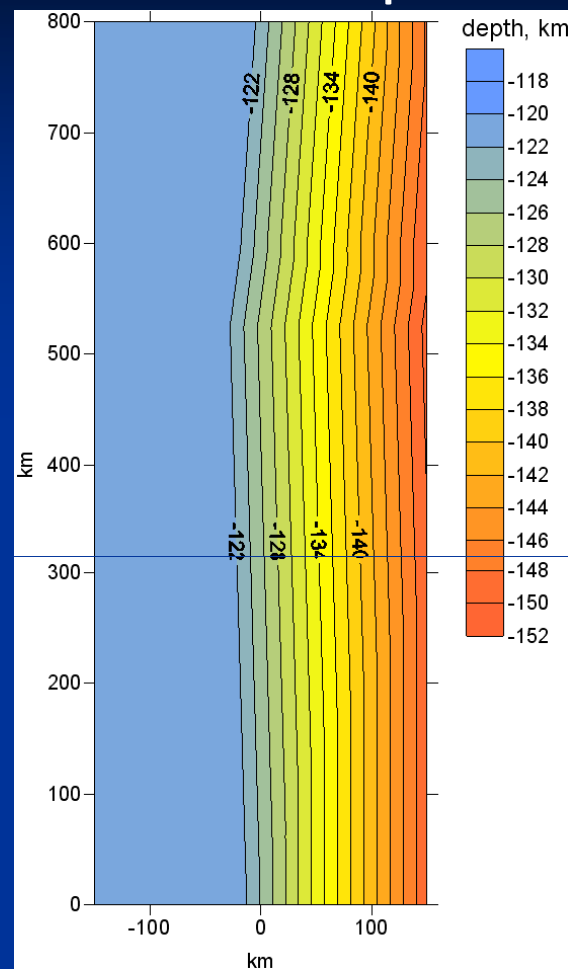
Flat Earth  
approximation

# Initial lithospheric structure:

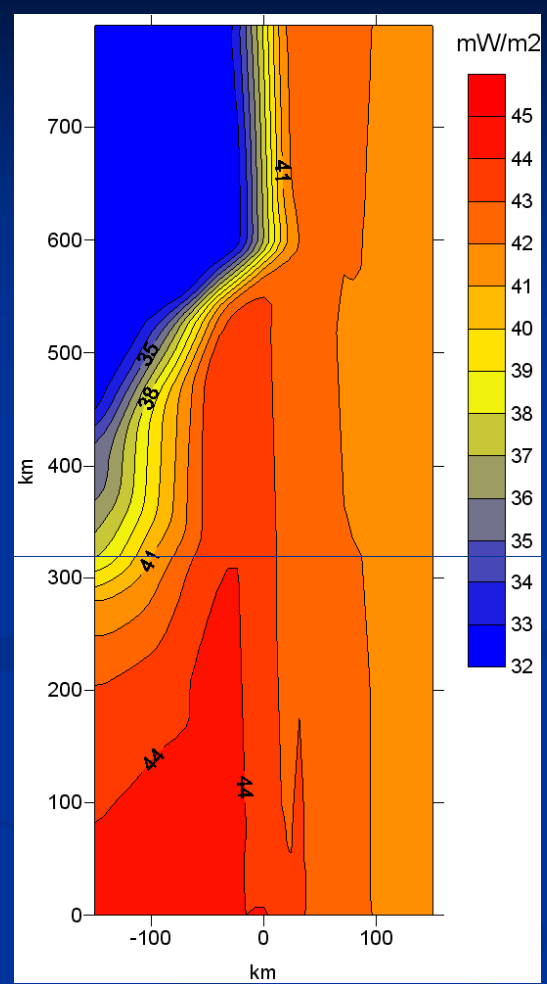
Moho map



LAB map

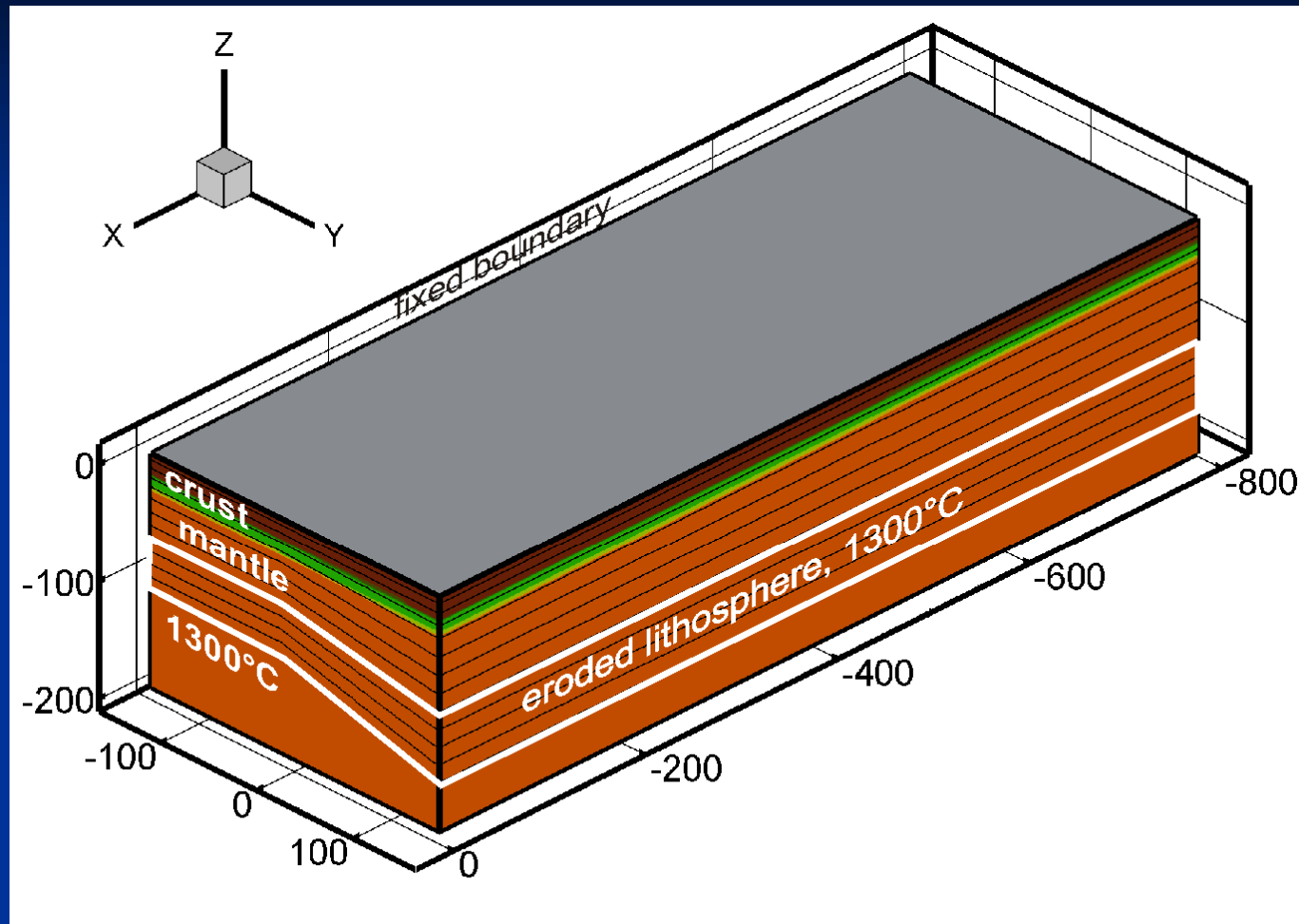


Heat flow

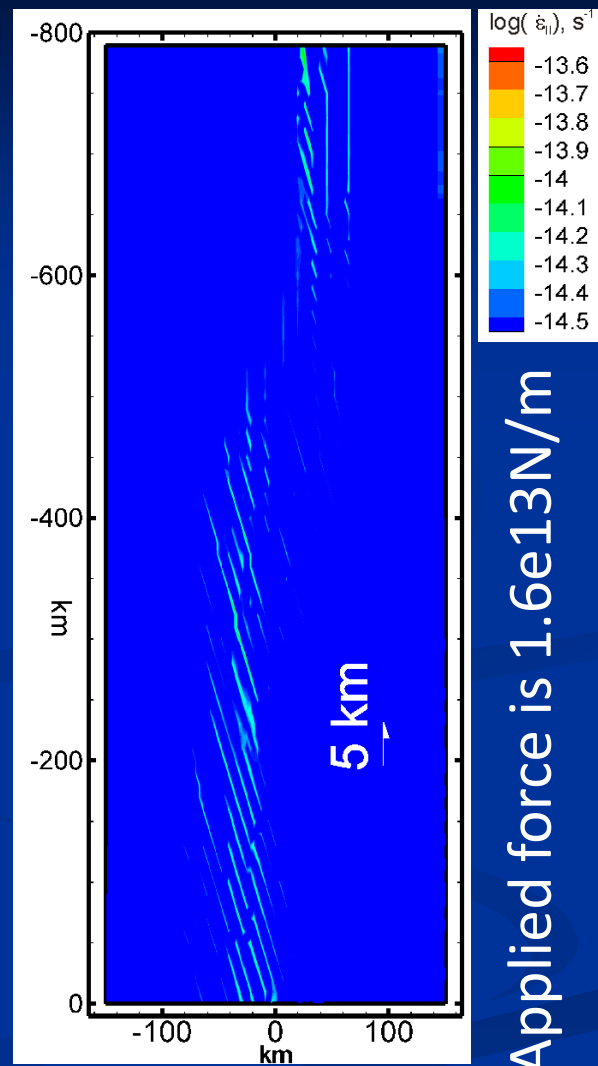
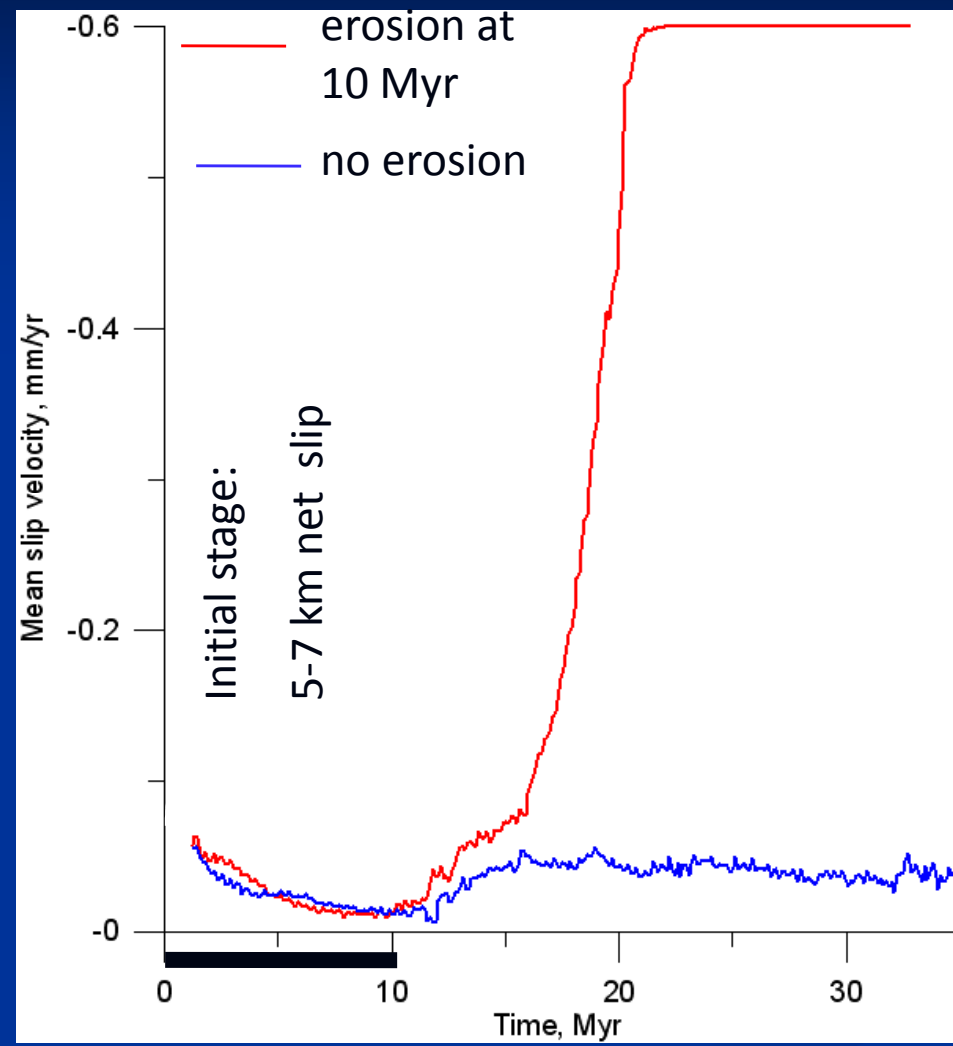


The region is characterized with the very low heat flow, of less than 55 mW/m<sup>2</sup>

# Assuming thermal erosion of the lithosphere



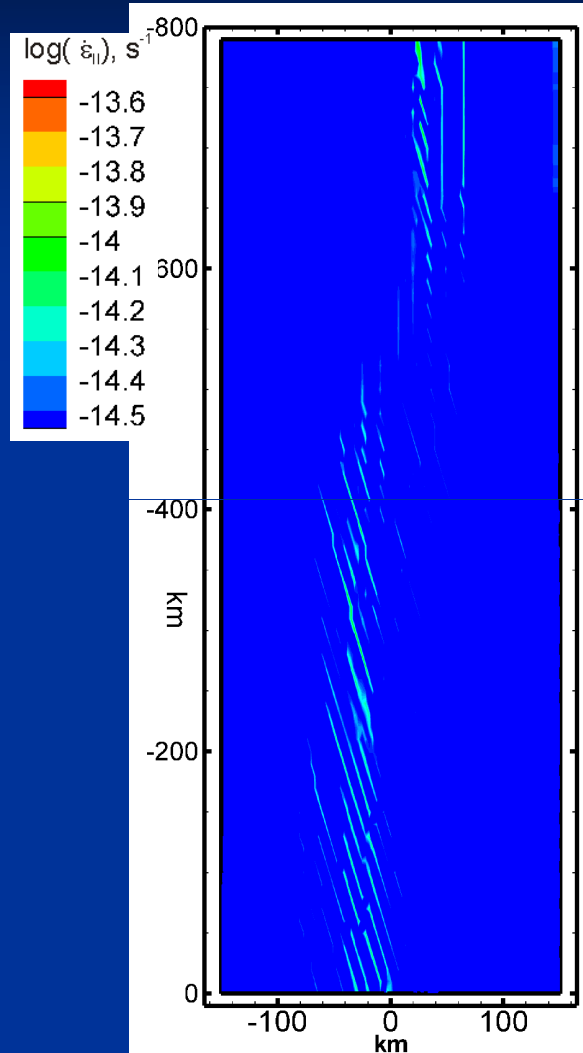
# 30-20 Ma rifting and beginning of opening of the Red Sea, thinning of the lithosphere in Saudi Arabia



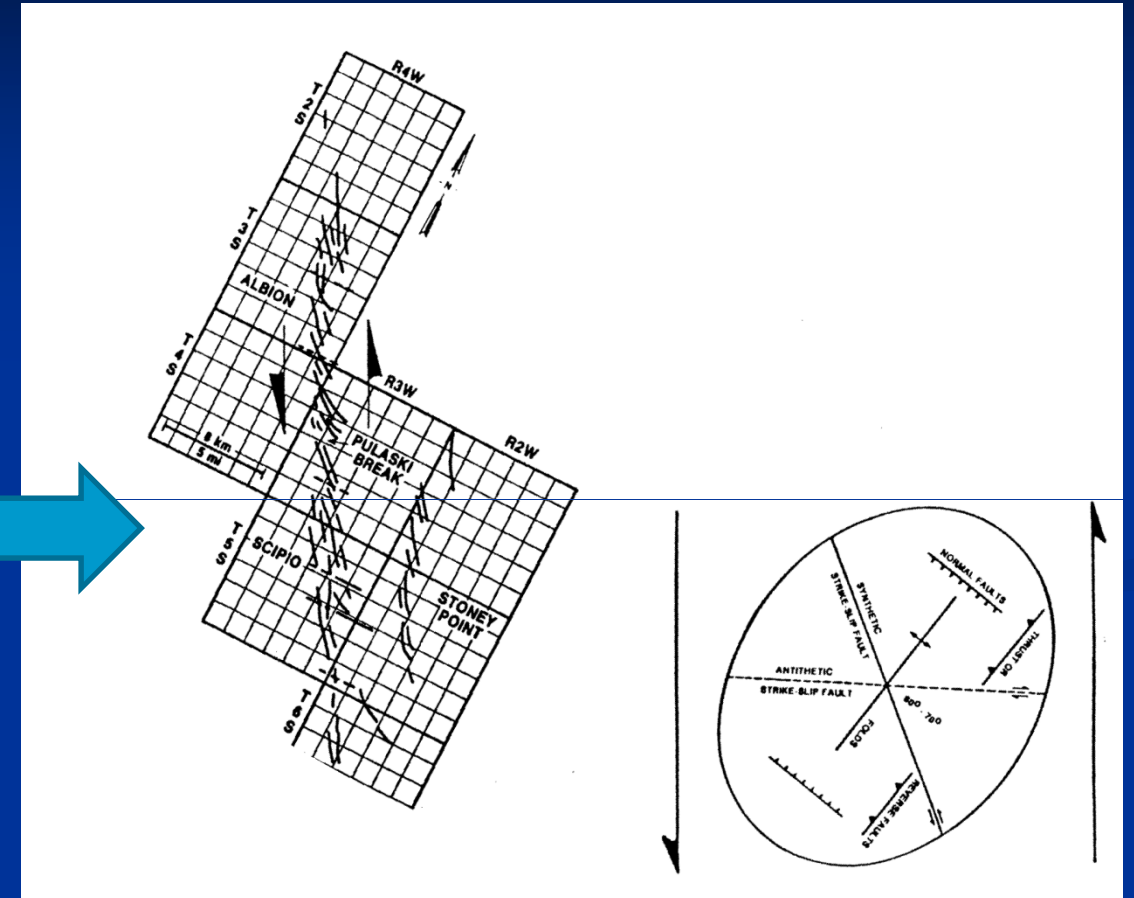
Applied force is  $1.6 \times 10^{13} N/m$

# Fault initiation

## Model example

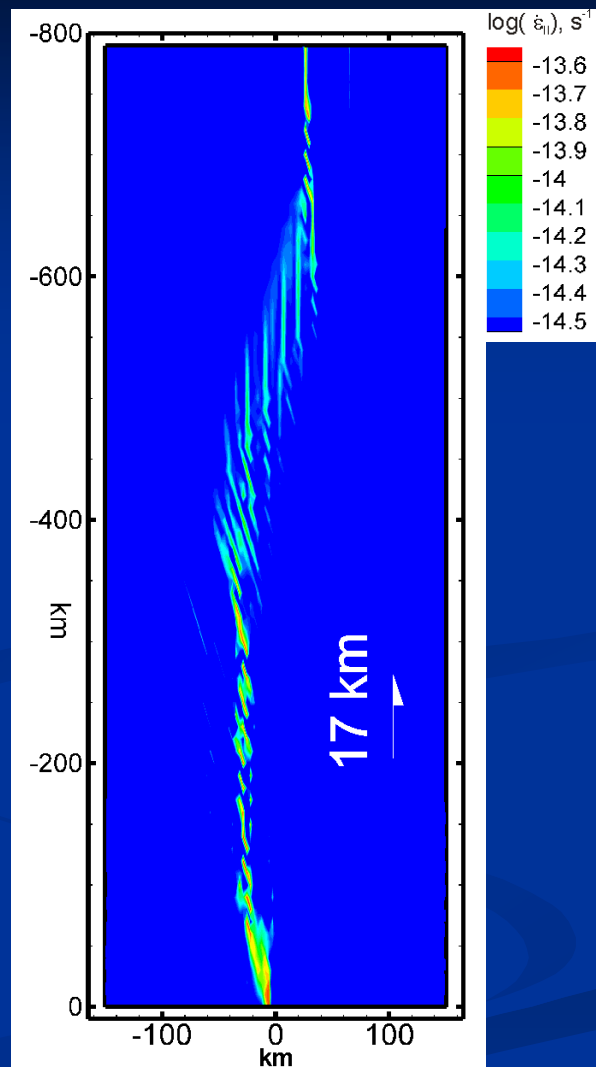
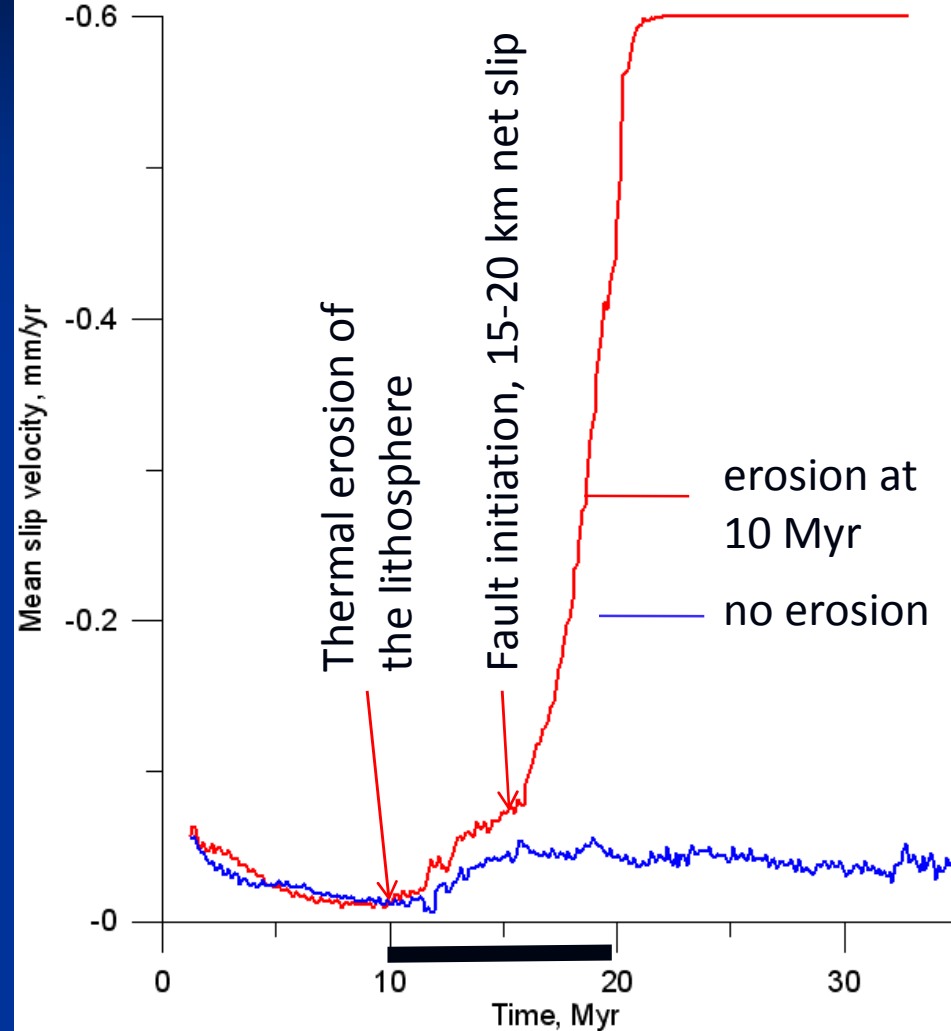


## Natural example

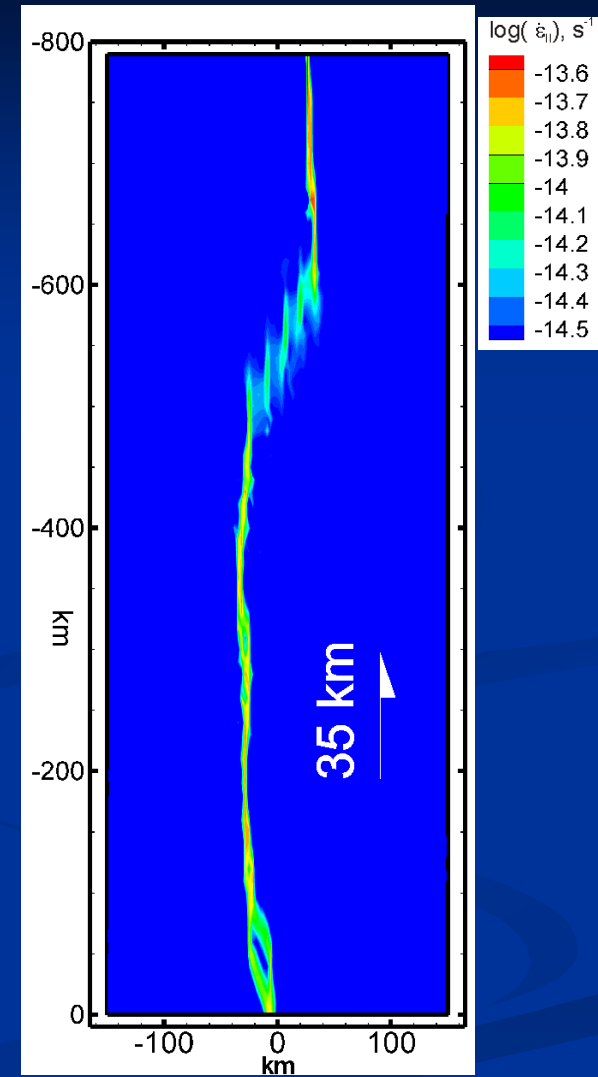
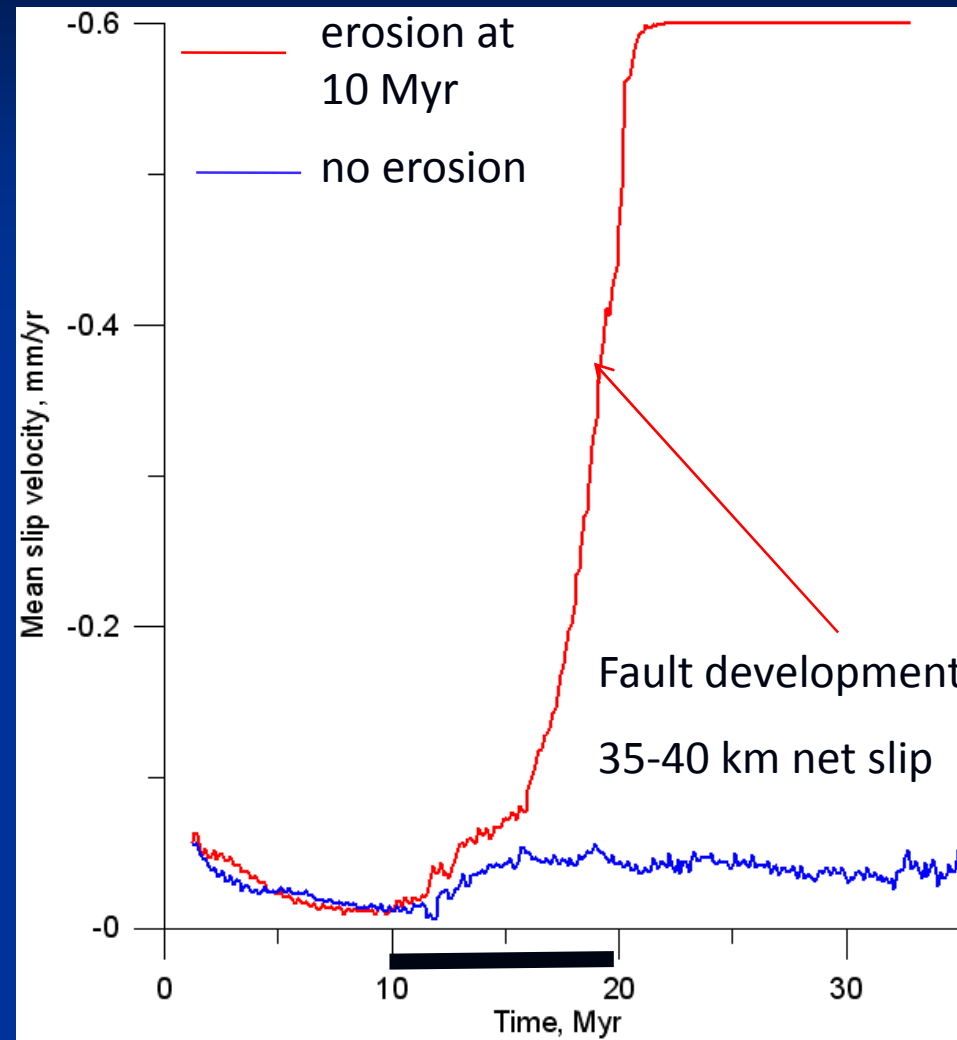


Albion-Scipio and Stoney Point Fields-U.S.A. Michigan Basin,  
From: Versical, 1991, M.S. Thesis, W.M.U

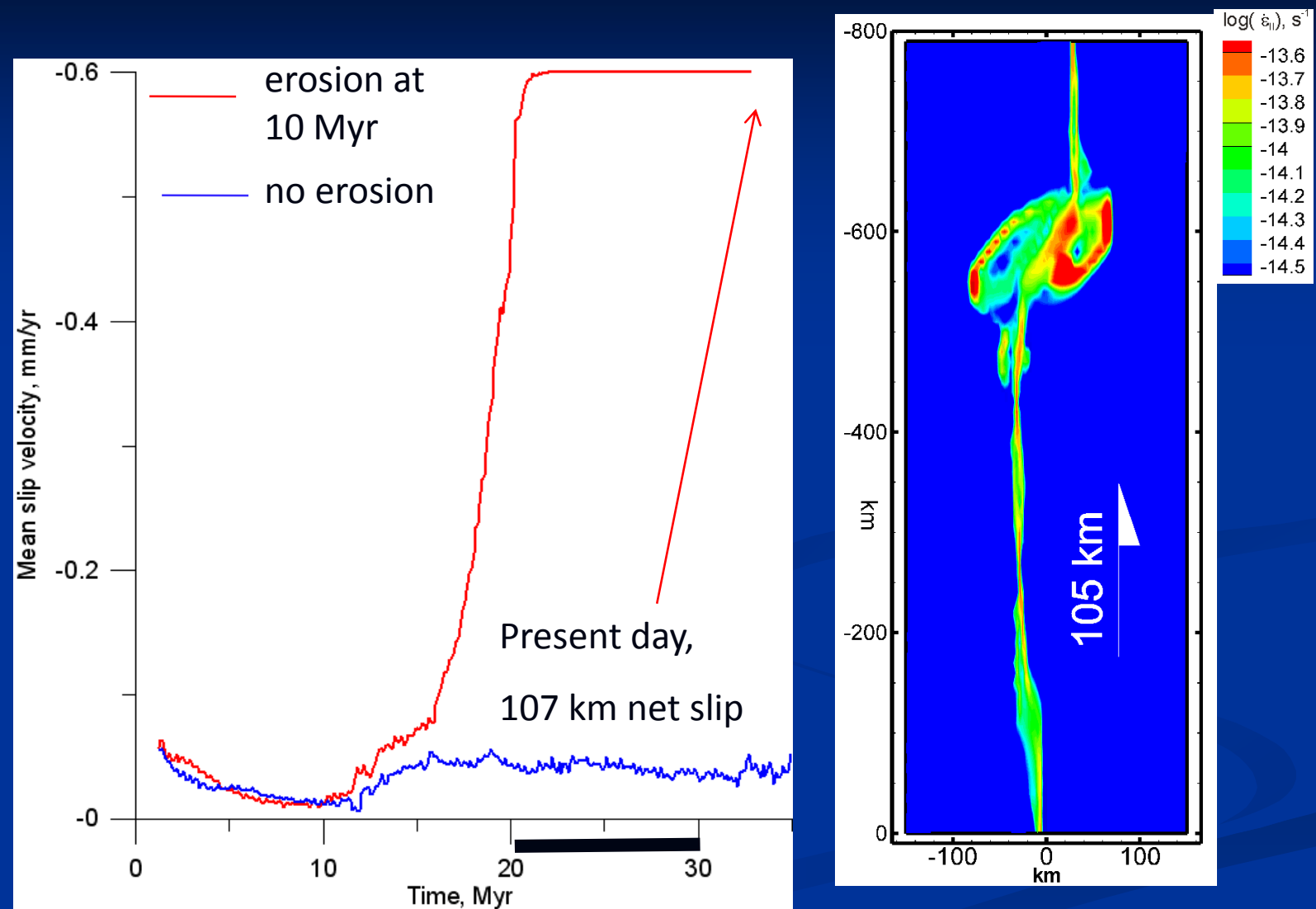
# 20-10 Ma thinning of the lithosphere around DST and localization of the DST



# 20-10 Ma thinning of the lithosphere around DST and localization of the DST

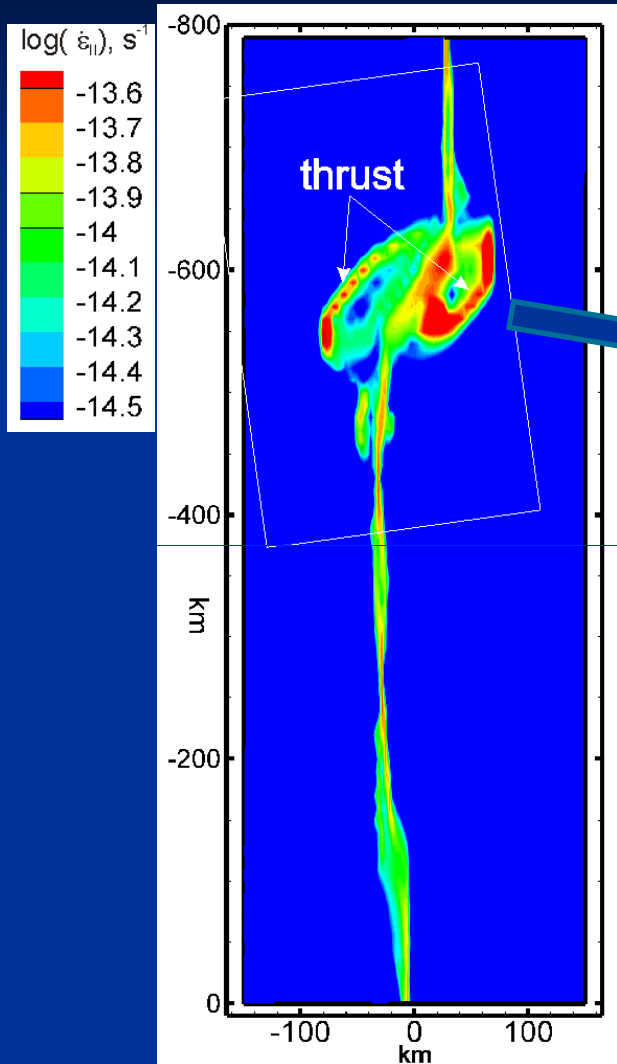


# 10-0 Ma mature DST, transpression and thrusting in Lebanon

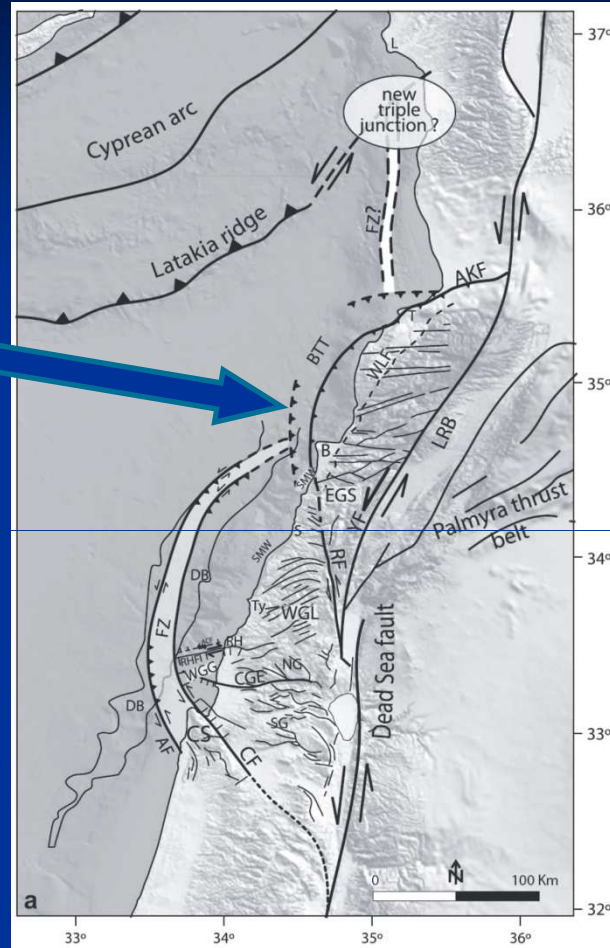


# Lebanon Mountains structure

## Model example



## Natural example



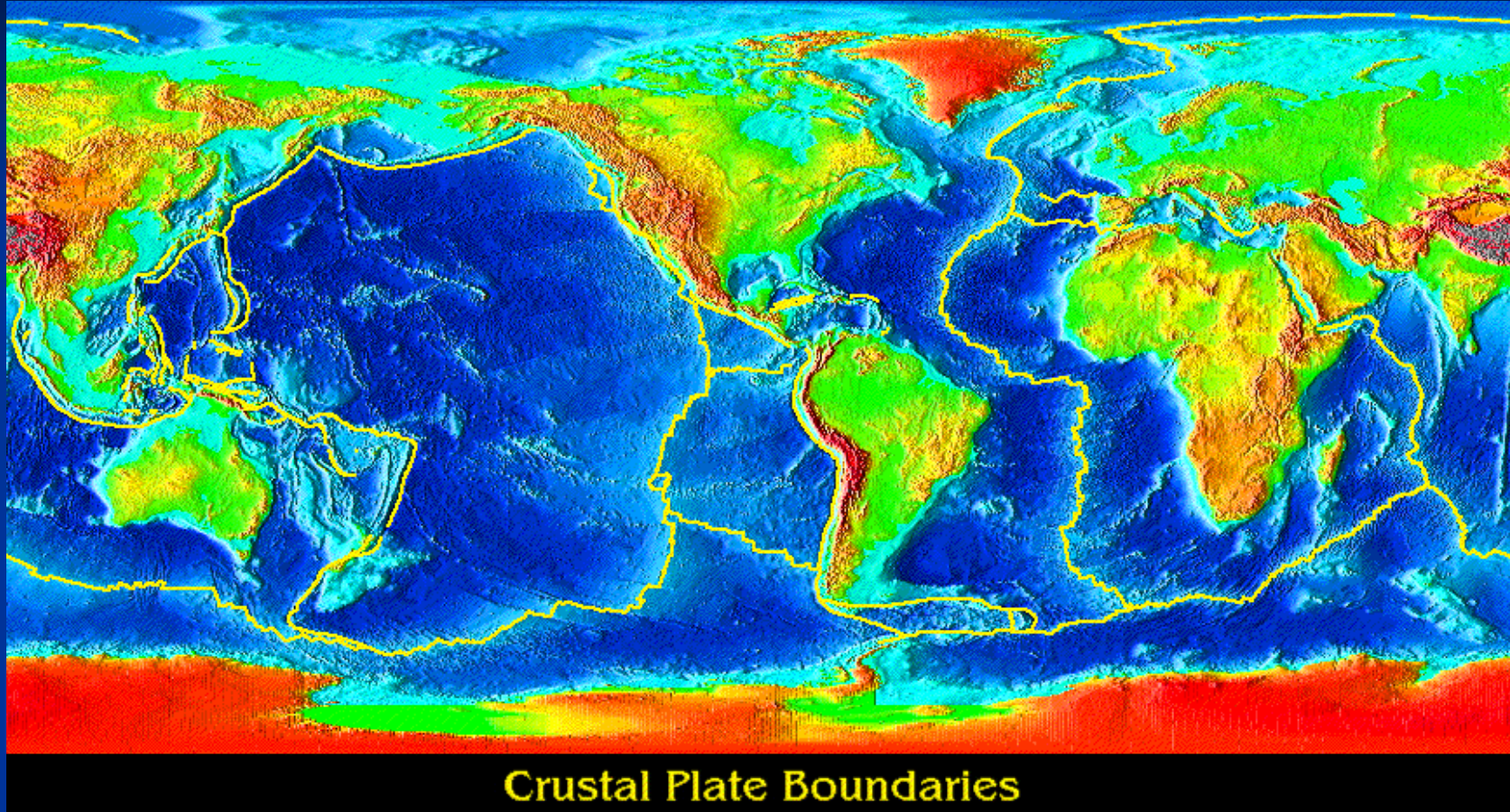
Map summarizing the main tectonic elements  
of the Lebanon Mountains (Schattner et al., 2006)

# Conclusion

The DST has likely originated through “cooperation” of the plate-tectonic scale forces and Afar plume, which has thinned lithosphere at and around the Red Sea and triggered strain localization at the DST

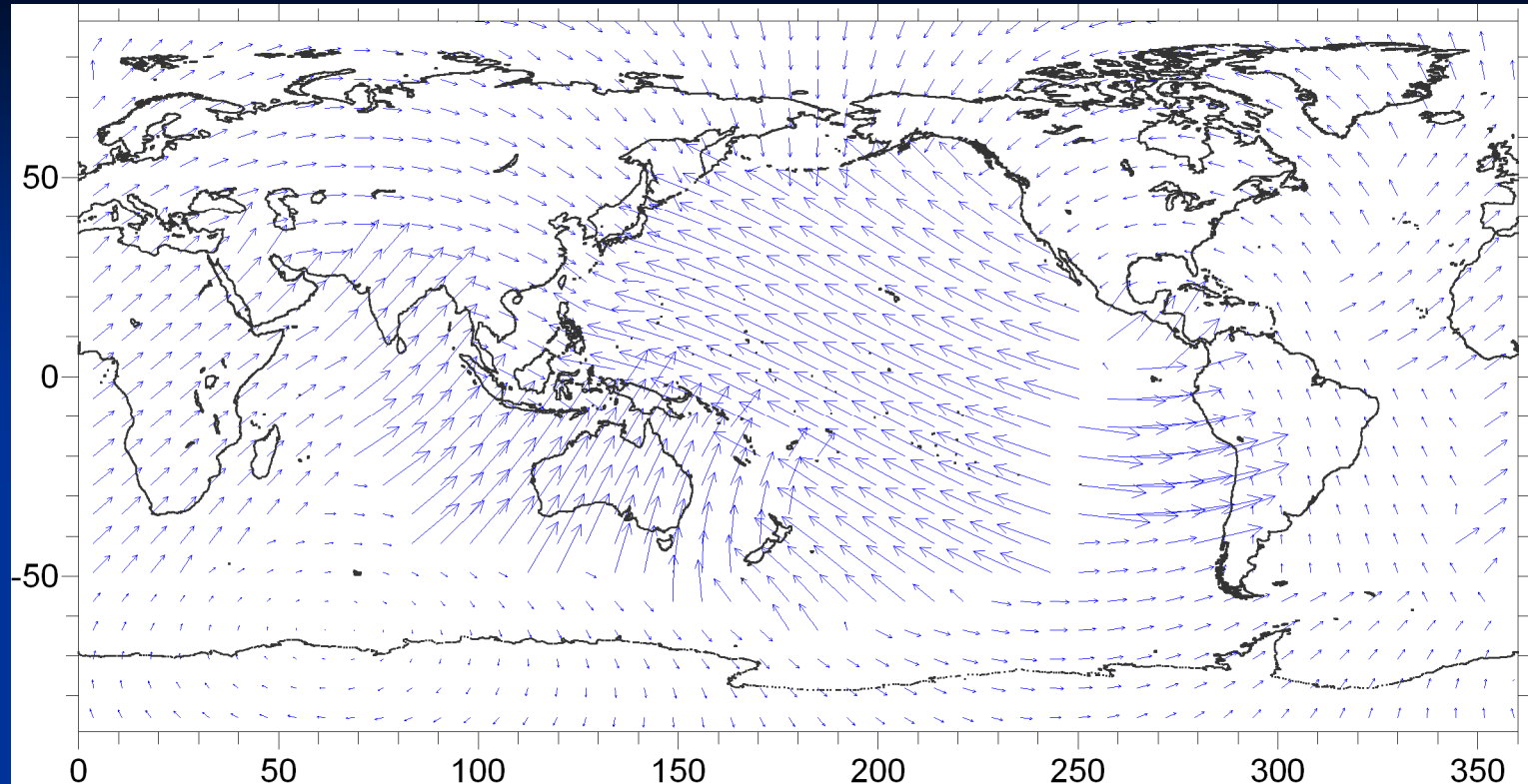
# Modeling Plate Velocities

(In cooperation with A. Popov and B. Steinberger)



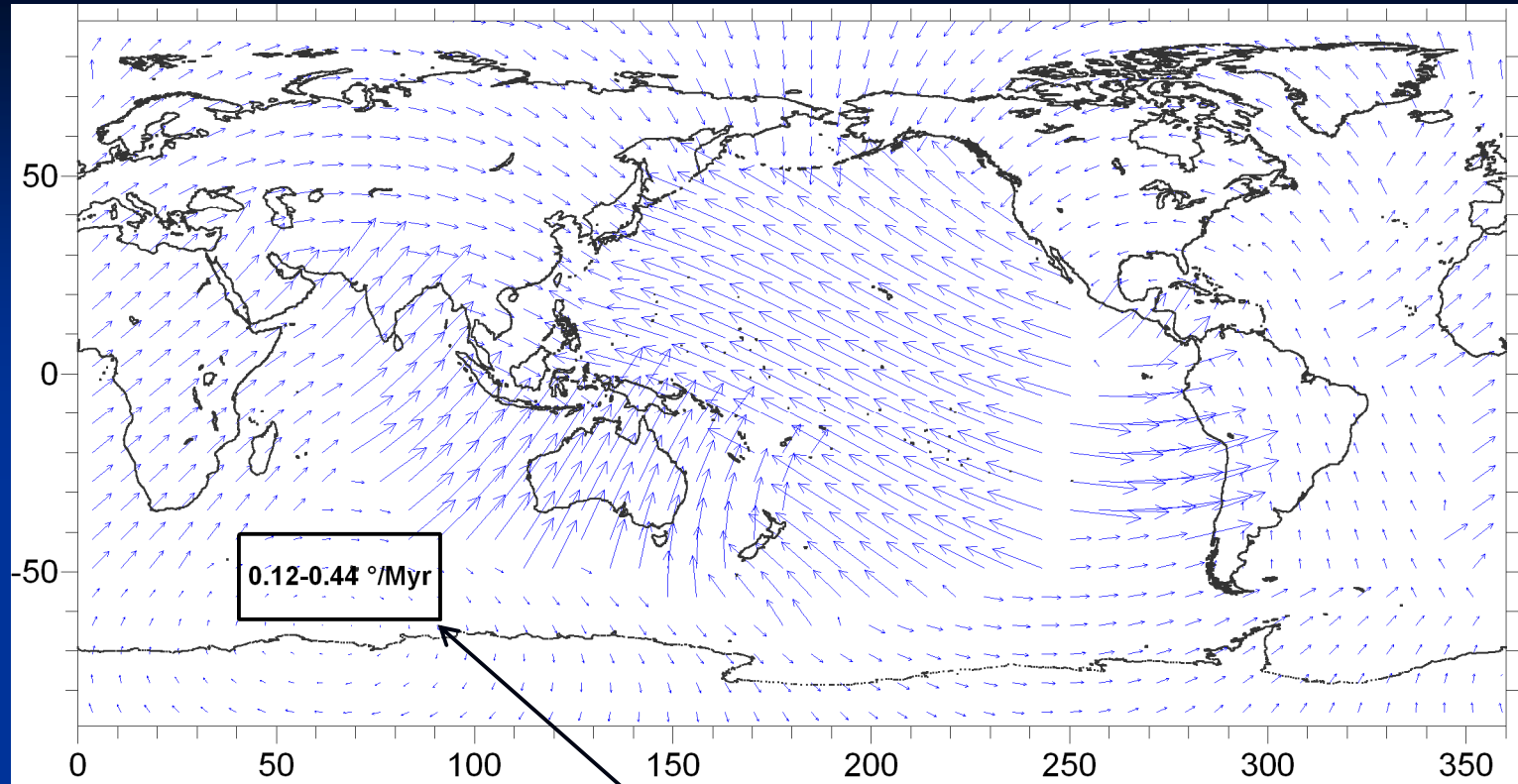
How weak are plate boundaries and how  
wet is the asthenosphere?

# Plate velocities



Observed plate velocities in no-net-rotation (NNR)  
reference frame

# Net rotation

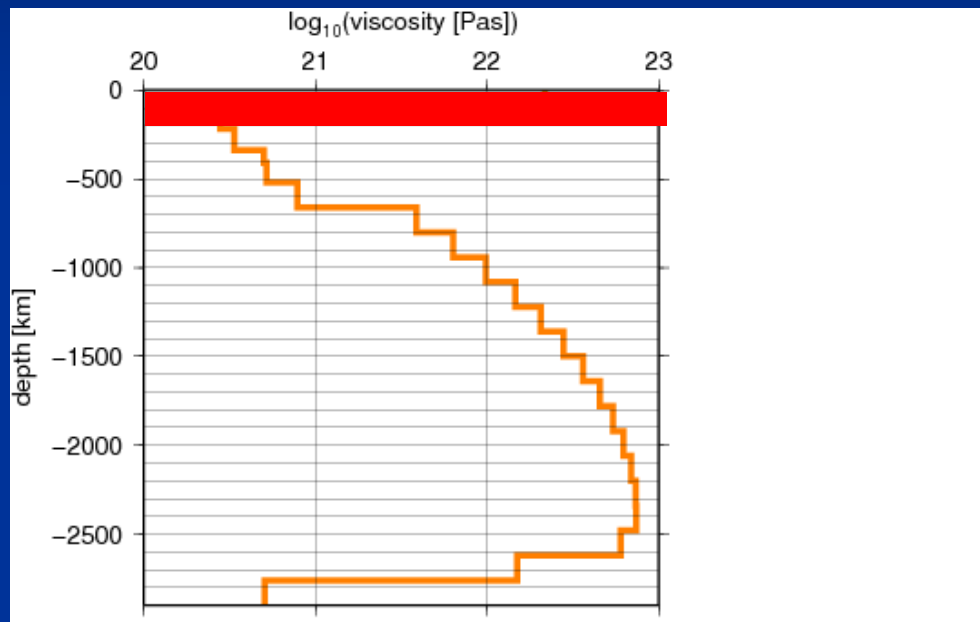


... and observed net-rotation (NR) of the lithosphere

Based on analyses of seismic anisotropy Becker (2008)  
narrowed possible range of angular NR velocities down to  
0.12-0.22 °/Myr

## Above 300 km depth

3D temperature and crust, numerical FEM technique  
(Popov and Sobolev, 2008) with **3D temperature- and stress-dependant visco-elasto-plastic rheology**



and **3D density distributions** based on subduction history  
(Steinberger, 2000)

## Below 300 km depth

Spectral method (Hager and O'Connell, 1981) with **radial viscosity distribution** from Steinberger and Calderwood (2006)

# Mantle rheology

**Mantle lithosphere:** dry olivine rheology combining diffusion and dislocation creep

$$\dot{\varepsilon}_H = Ad^{-m} \sigma_H^n \exp(-(E_a + PV_a)/RT)$$

**Asthenosphere:** wet olivine rheology combining diffusion and dislocation creep with water content as model parameter

$$\dot{\varepsilon}_H = Ad^{-m} C_{H_2O}^p \sigma_H^n \exp(-(E_a + PV_a)/RT)$$

Parameters in reference model by Hirth and Kohlstedt (2003) with n=3.5 +-0.3 and activation volume from Kawazoe et al. (2009).

Modifications according to

$$\dot{\varepsilon}_H(n) = \dot{\varepsilon}_H(n_{ref}) (\sigma_H / 100 MPa)^{n-n_{ref}}$$

# Plate boundaries

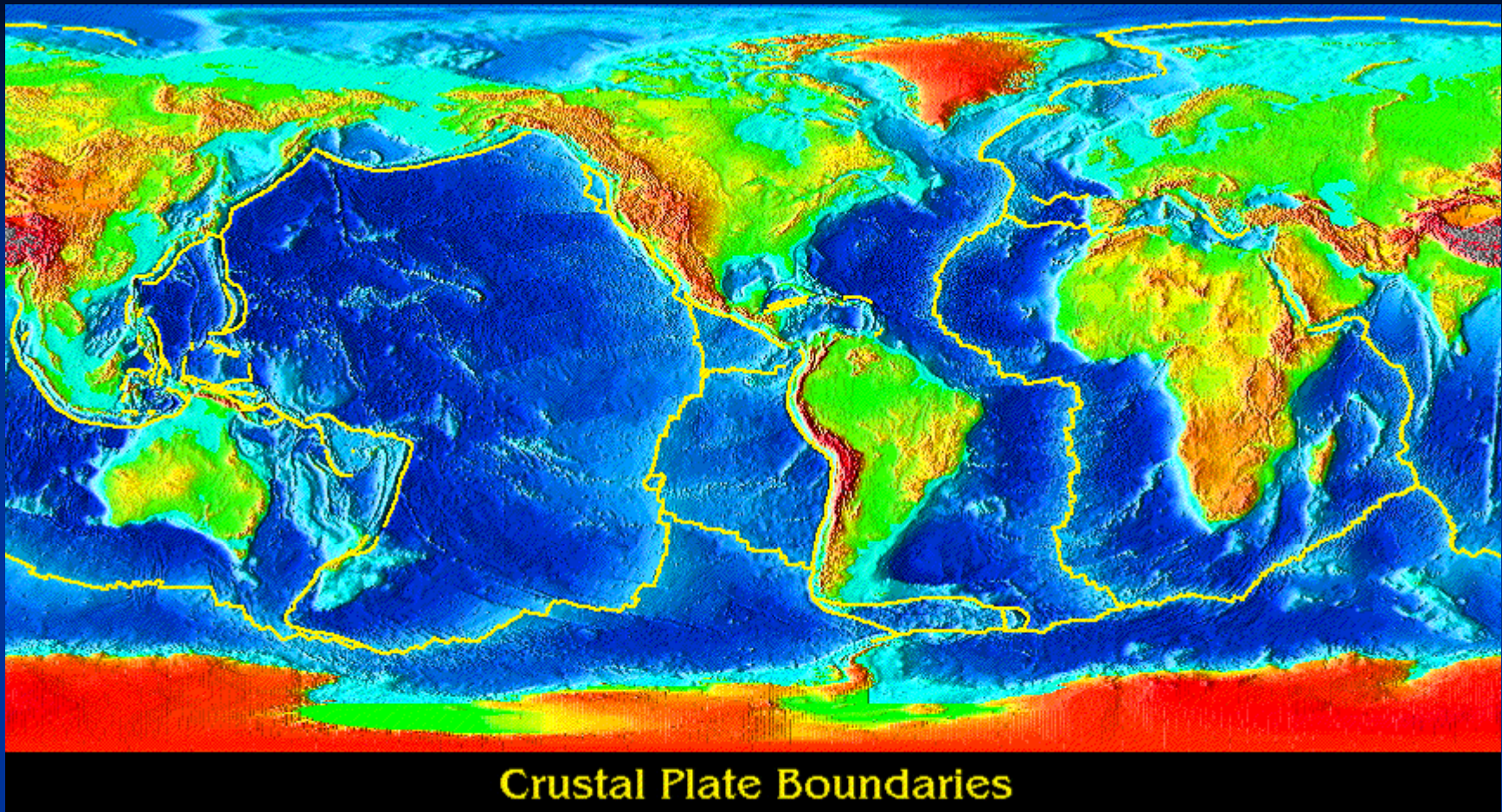
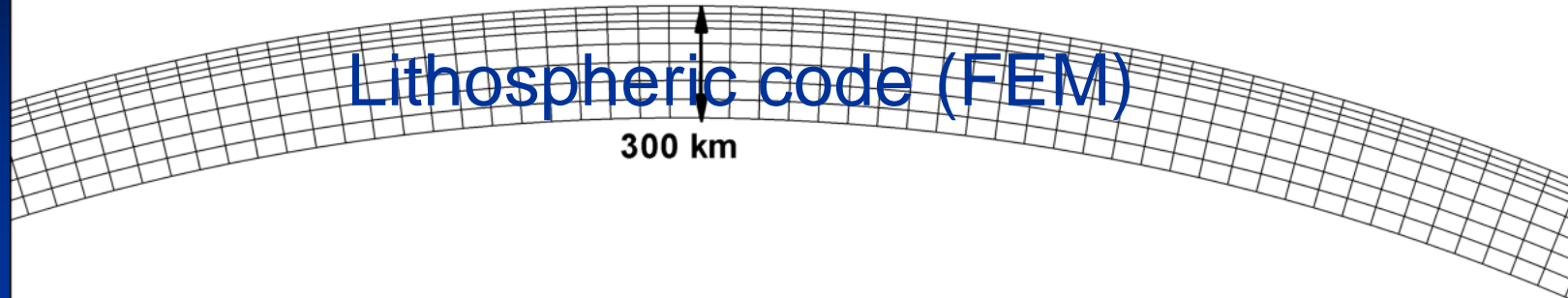


Plate boundaries are defined as narrow zones with visco-plastic rheology where friction coefficient is model parameter

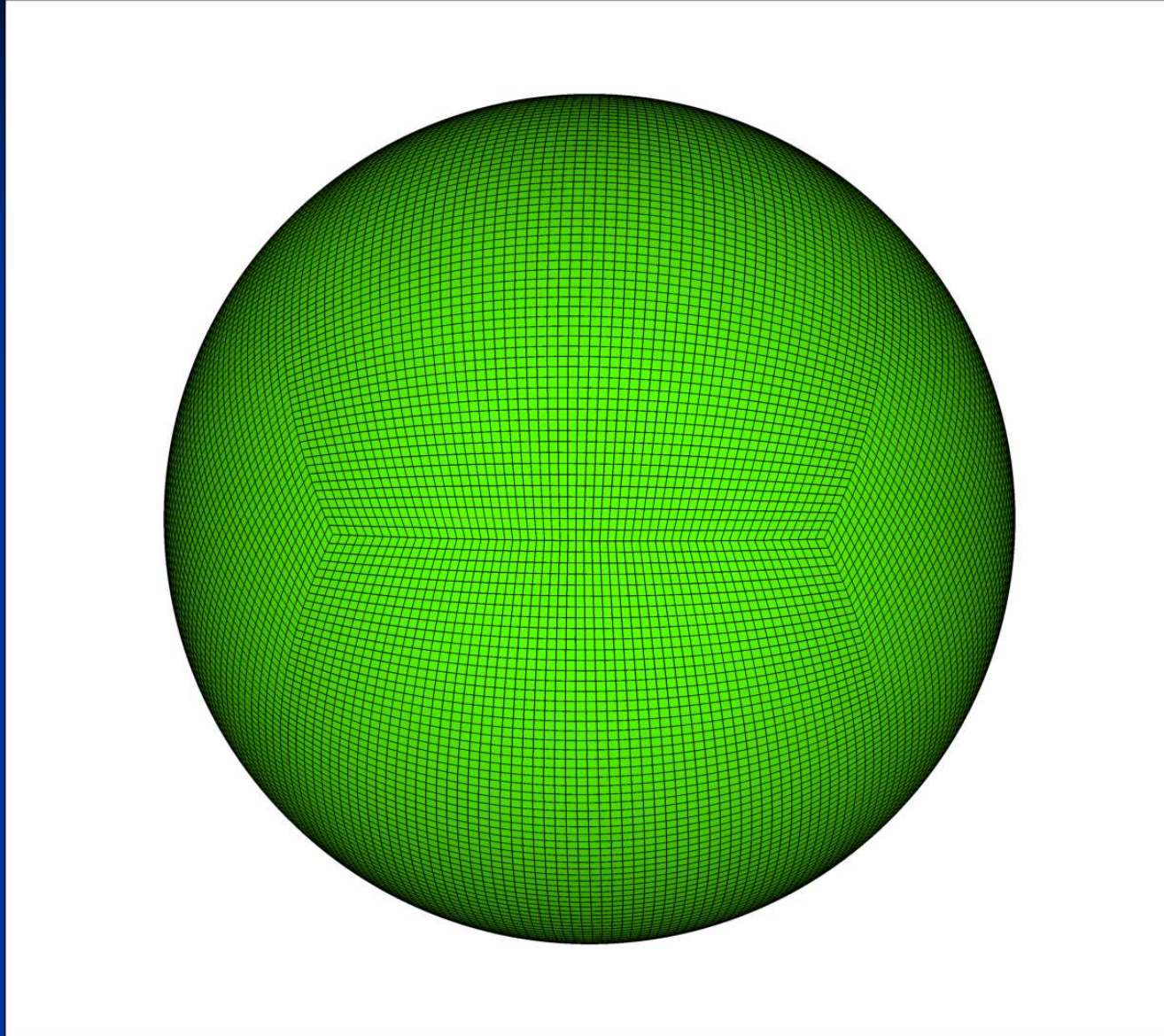


## Mantle code (spectral)

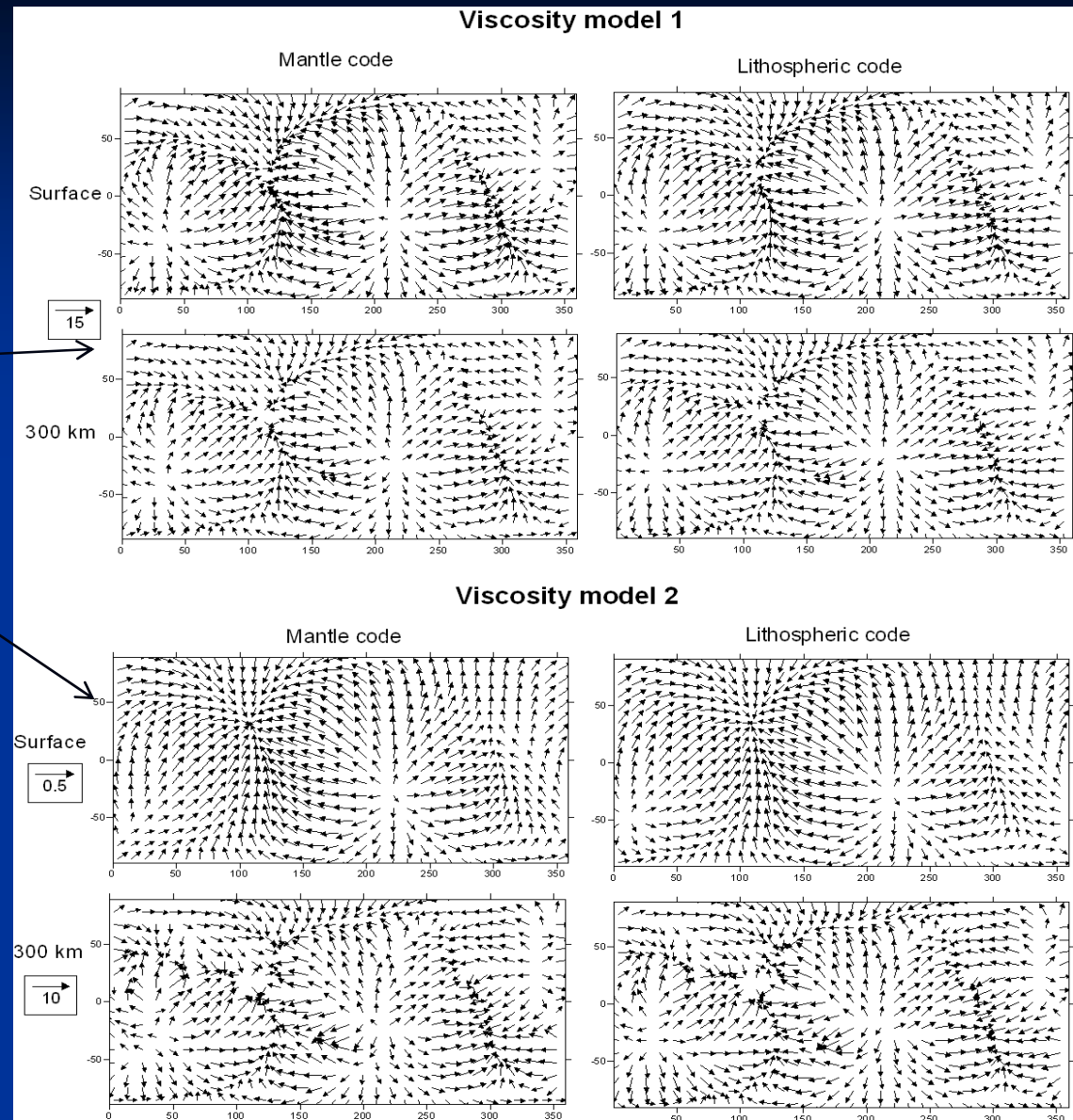
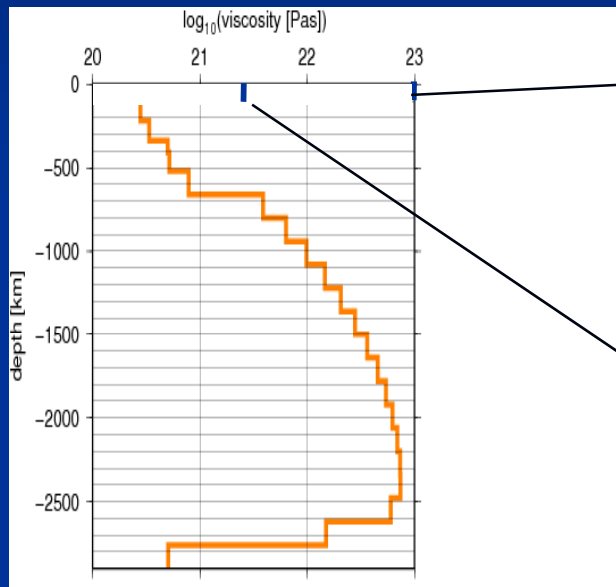
Mantle and lithospheric codes are coupled through continuity of velocities and tractions at 300 km.

The model has free surface and 3D, strongly non-linear visco-elastic rheology with true plasticity (brittle failure) in upper 300km.

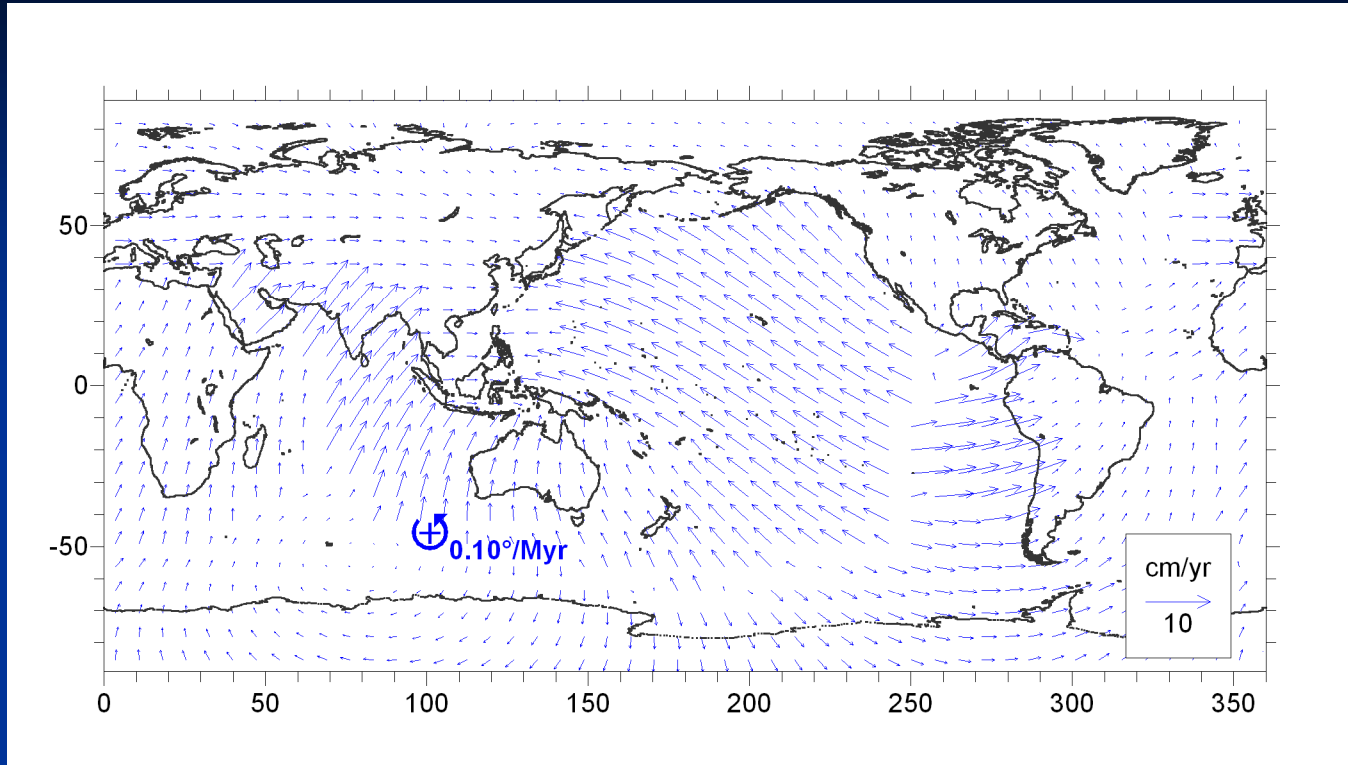
# Mesh for low-resolution model



# Benchmark test

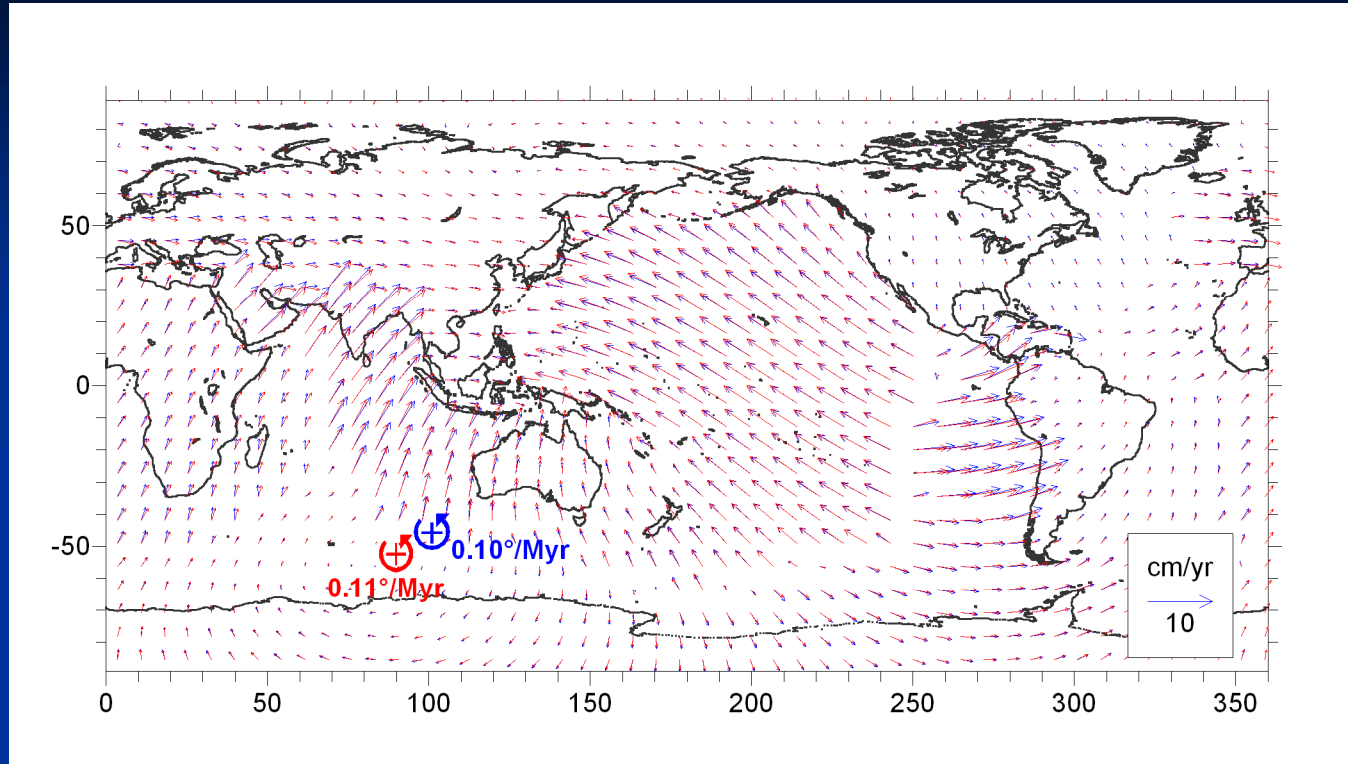


# Model by Becker (2006)



CitcomS, 3-D temperature-dependant dislocation+diffusion rheology, **lateral viscosity variations** in the entire mantle, low-viscosity plate boundaries

# Our model vrs. model by Becker (2006)



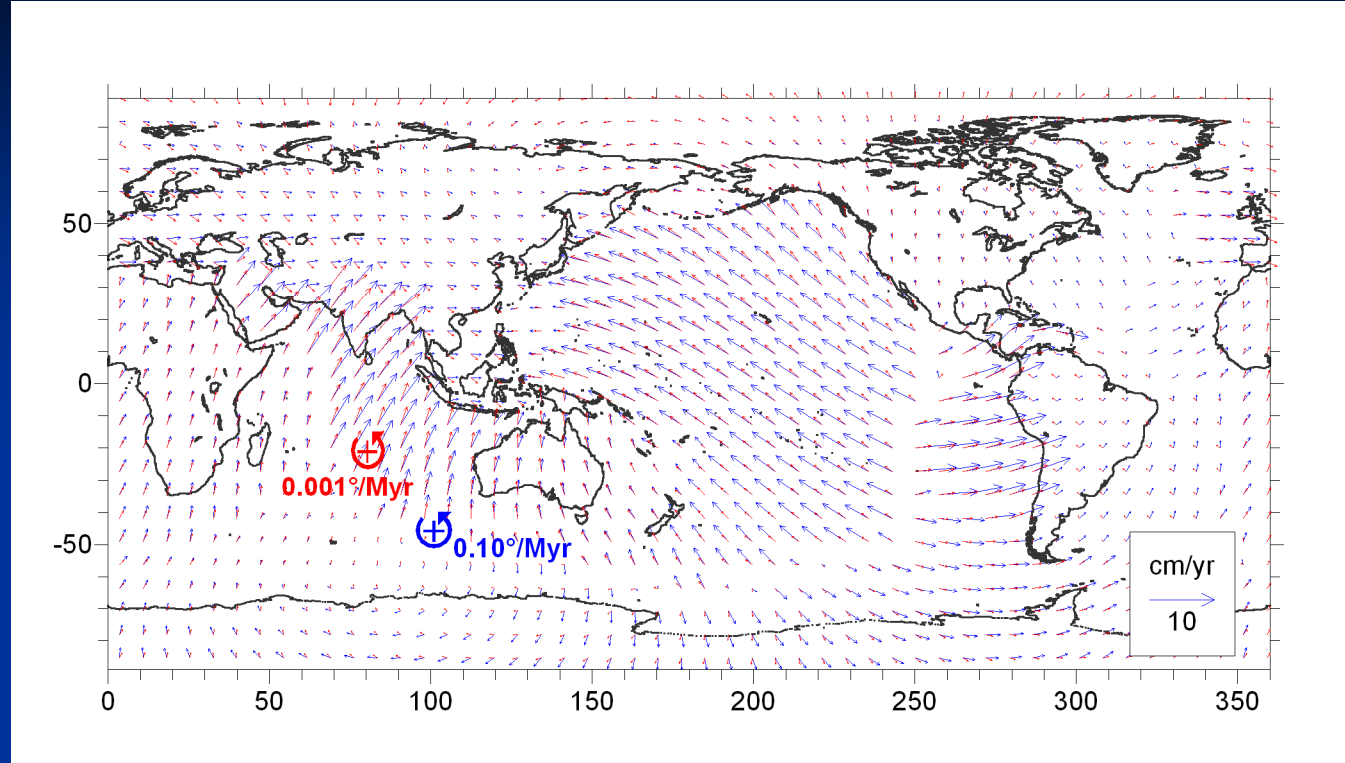
$$\text{Misfit} = \int \|\vec{v}_2 - \vec{v}_1\| / \|\vec{v}_1\| dS = 0.19$$

# Conclusion

Benchmark tests justify our hybrid-codes modeling approach and suggest that lateral viscosity variations **deeper than 300 km** may be ignored in modeling plate velocities

But what about lateral viscosity variations **shallower than 300 km?**

# Radial UM viscosity vrs. 3D UM viscosity



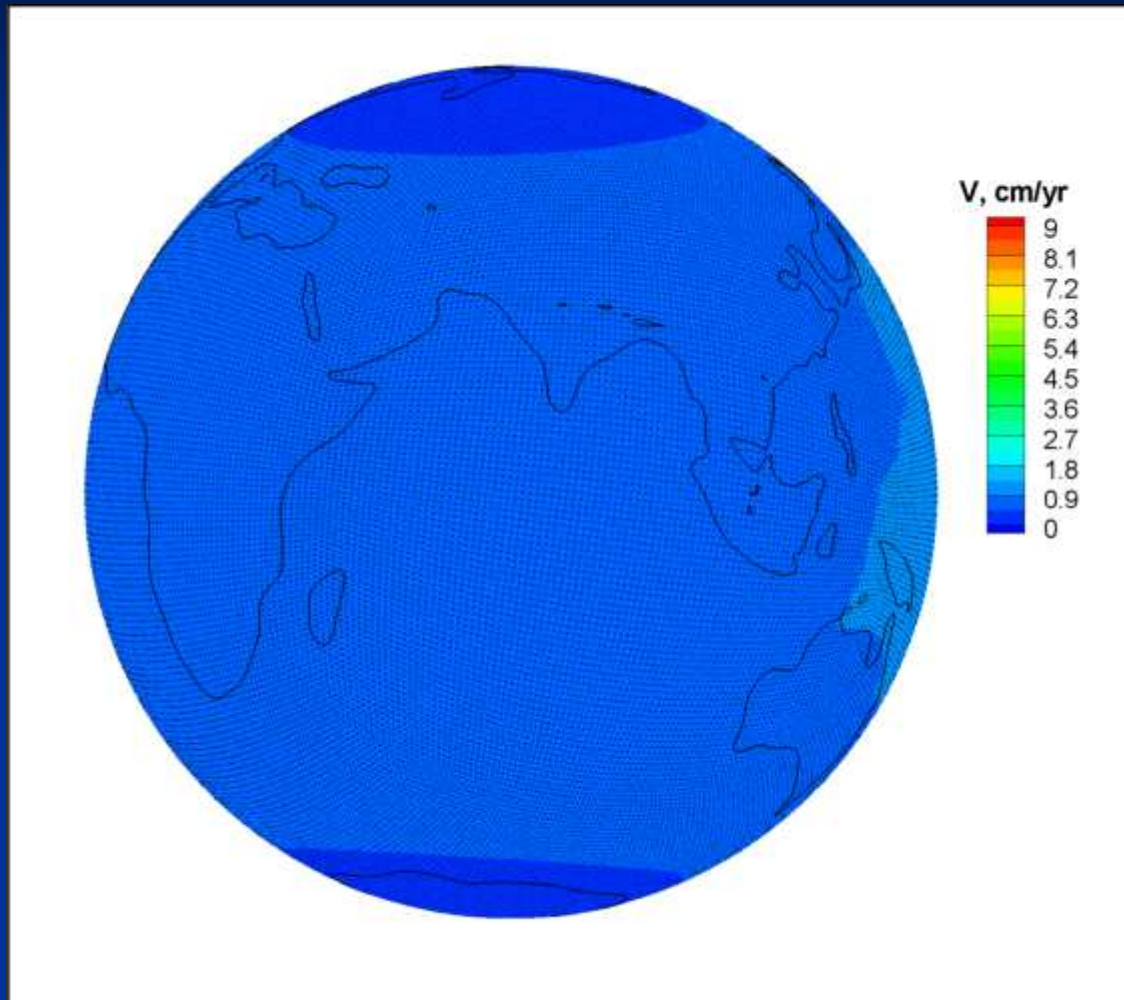
$$\text{Misfit} = \int \|\vec{v}_2 - \vec{v}_1\| / \|\vec{v}_1\| dS = 0.51$$

# Conclusion

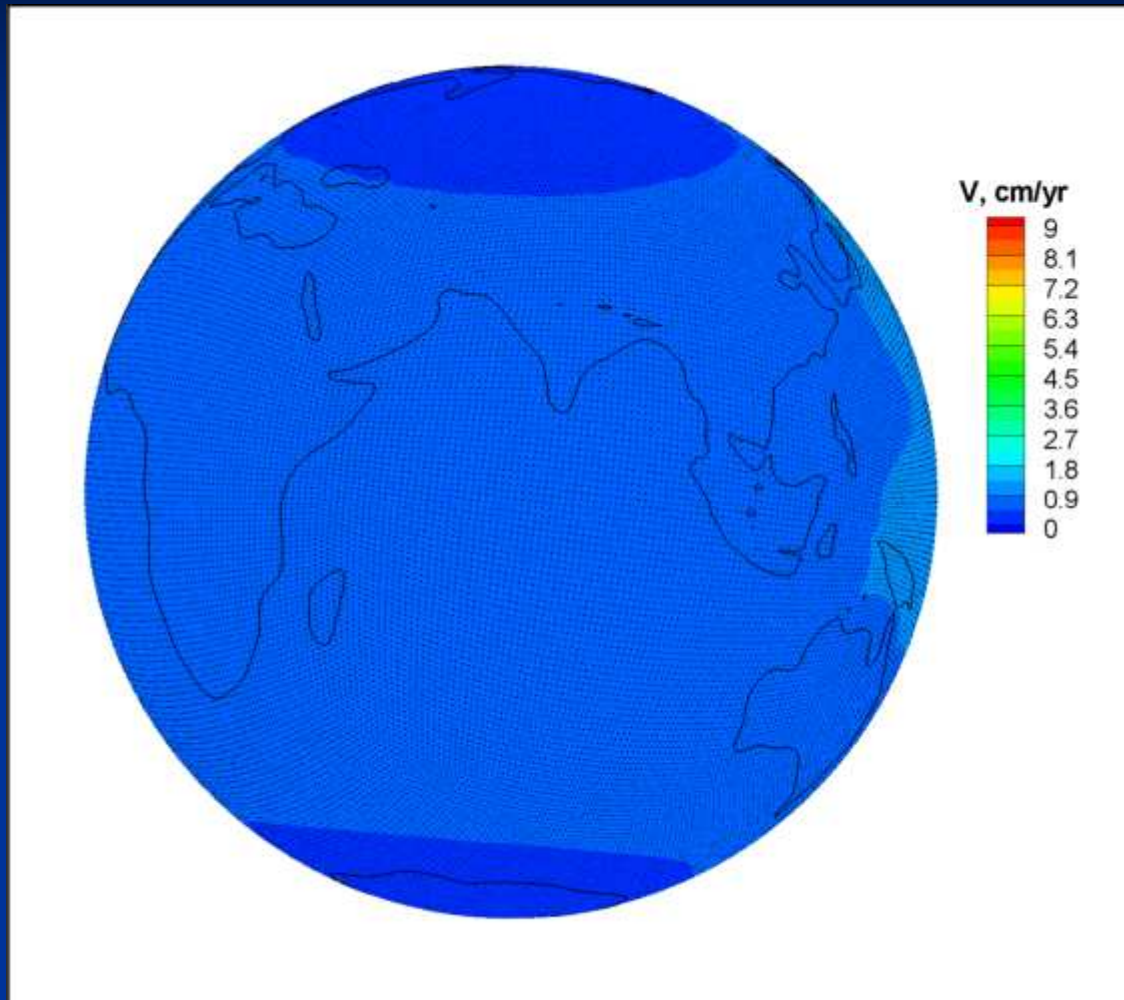
Lateral viscosity variations shallower than 300 km strongly affect magnitudes, but less directions of plate velocities

# Effect of strength at plate boundaries

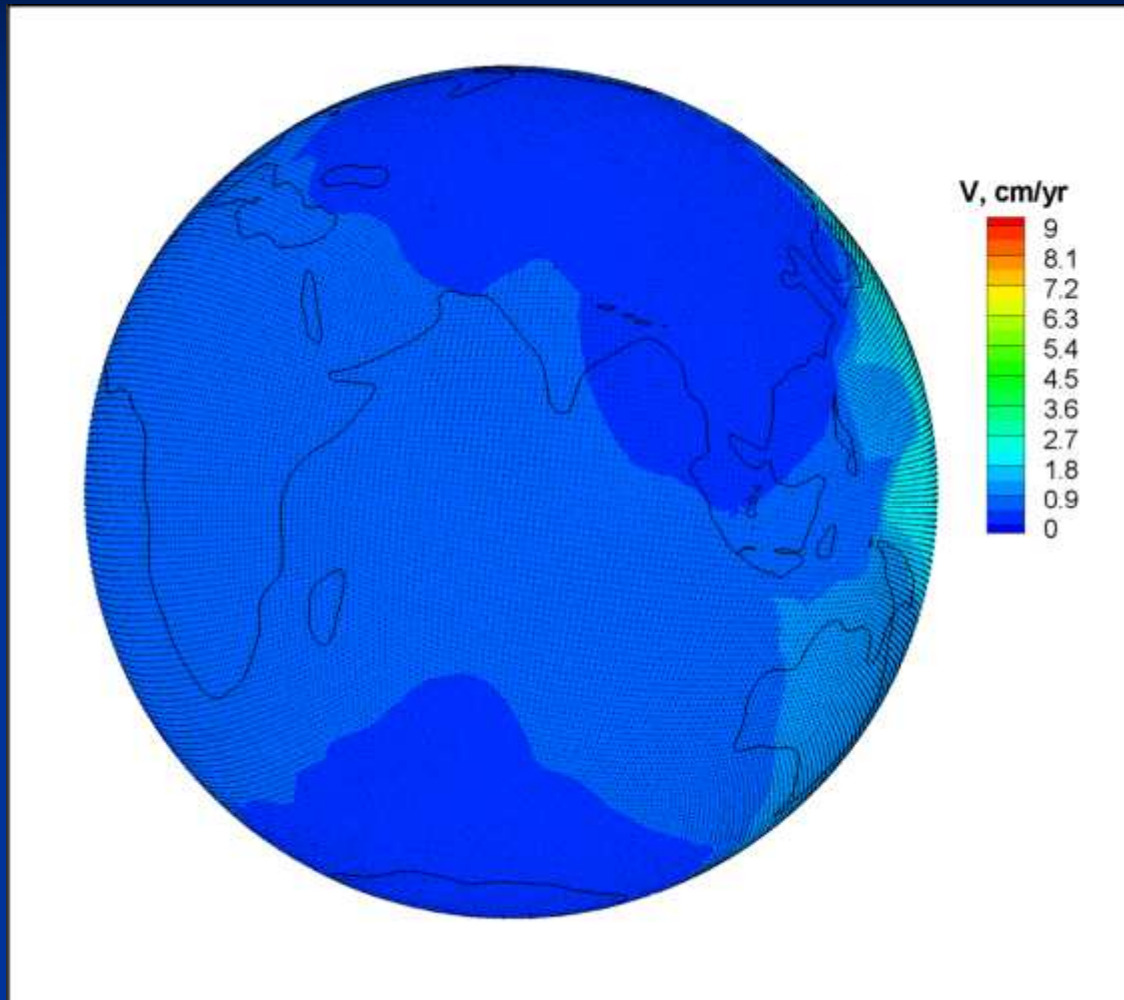
## Friction at boundaries 0.4



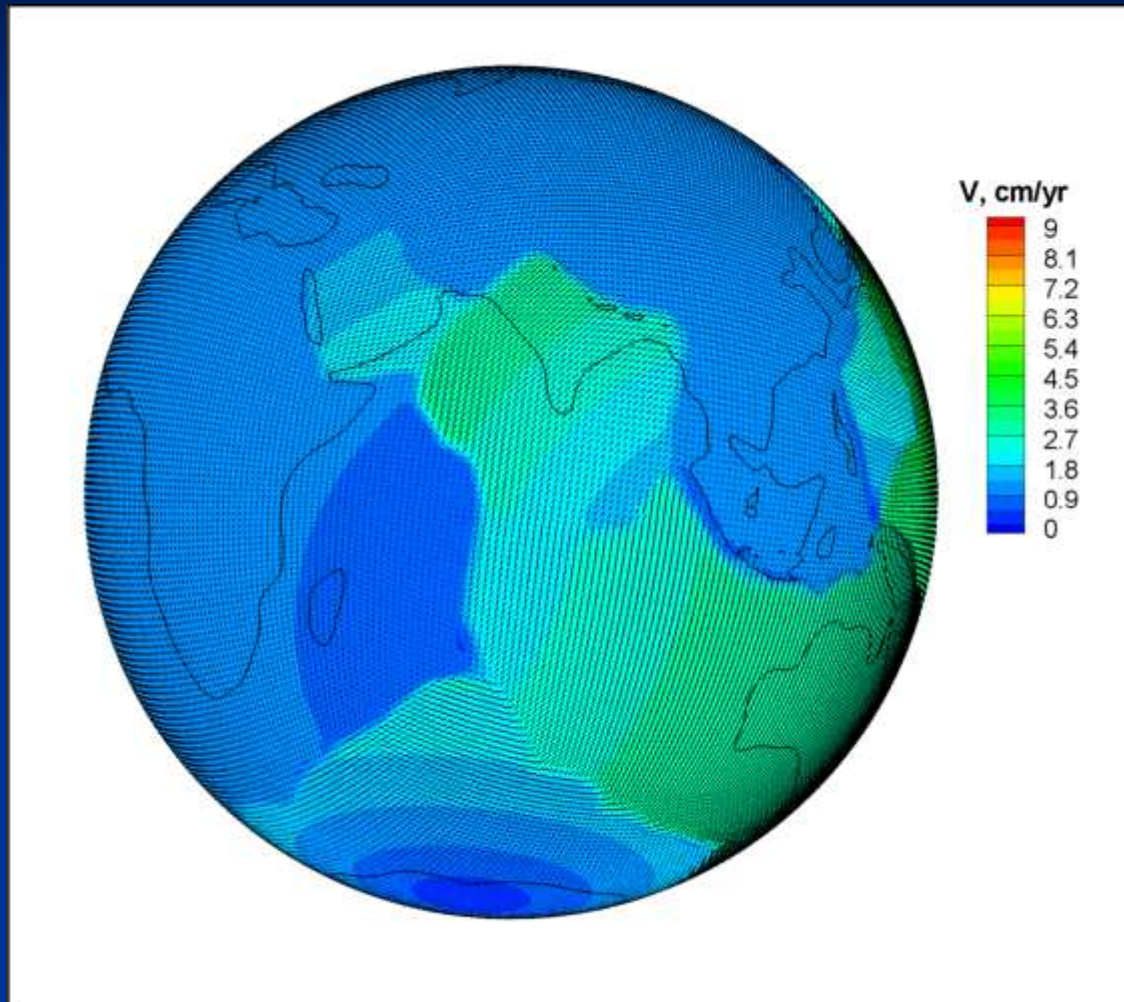
## Friction at boundaries 0.2



# Friction at boundaries 0.1

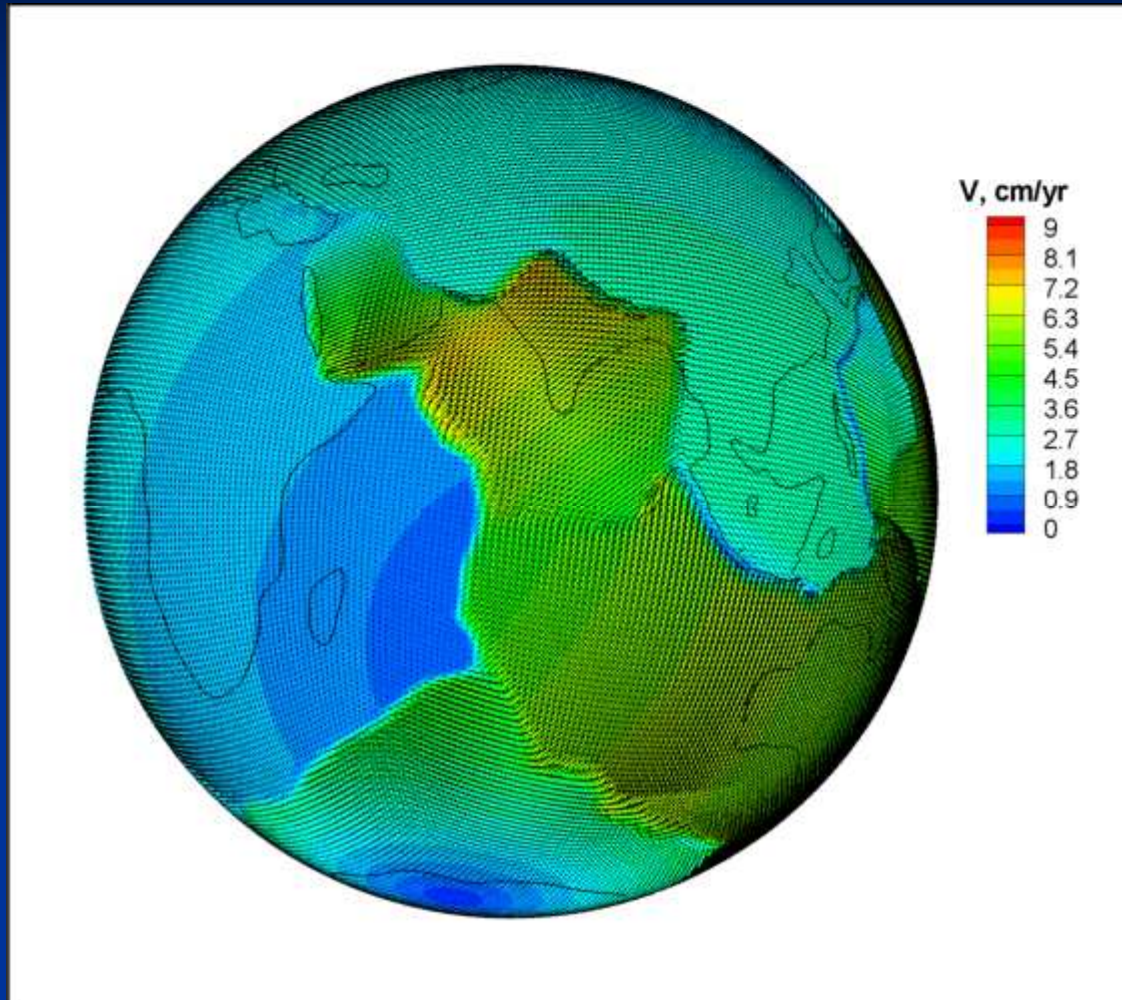


## Friction at boundaries 0.05



too low velocities

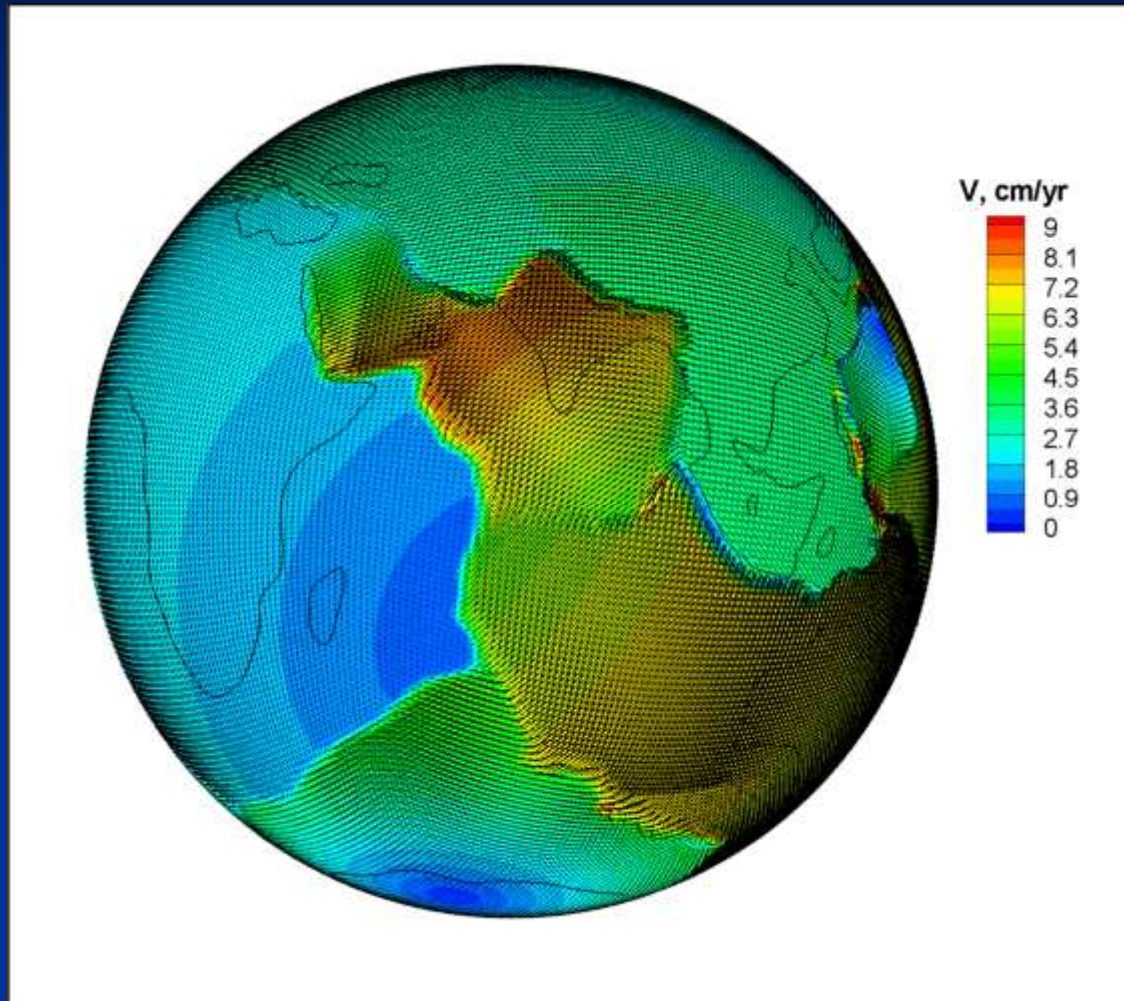
## Friction at boundaries 0.02



about right magnitudes of velocities

*Plates*

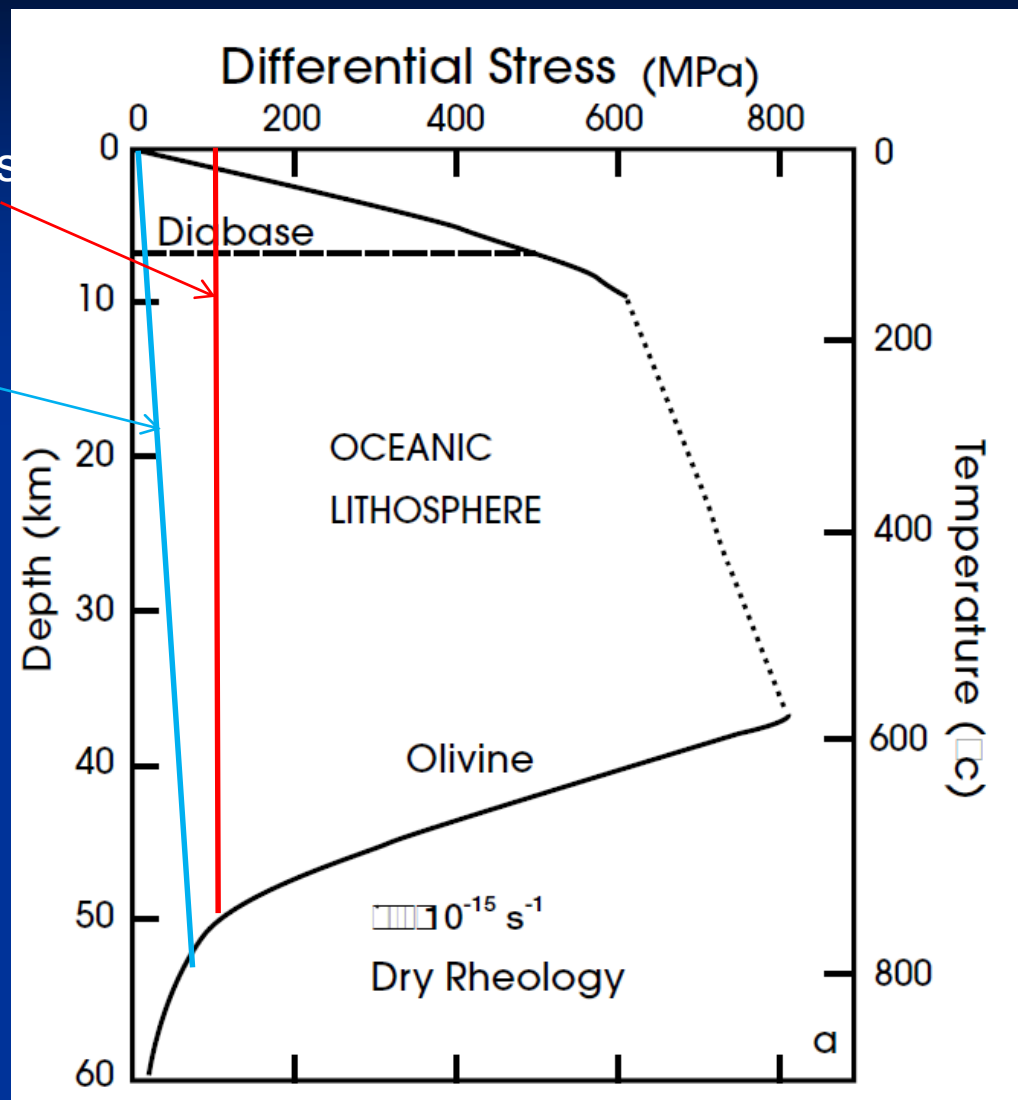
Friction at boundaries 0.01



too high velocities

# Weakness of the plate boundaries

Plate boundaries  
Tackley  
Plate boundaries  
this work



# Conclusion

Strength (friction) at plate boundaries strongly affect plate velocities and must be very low, much lower than measured for any dry rock

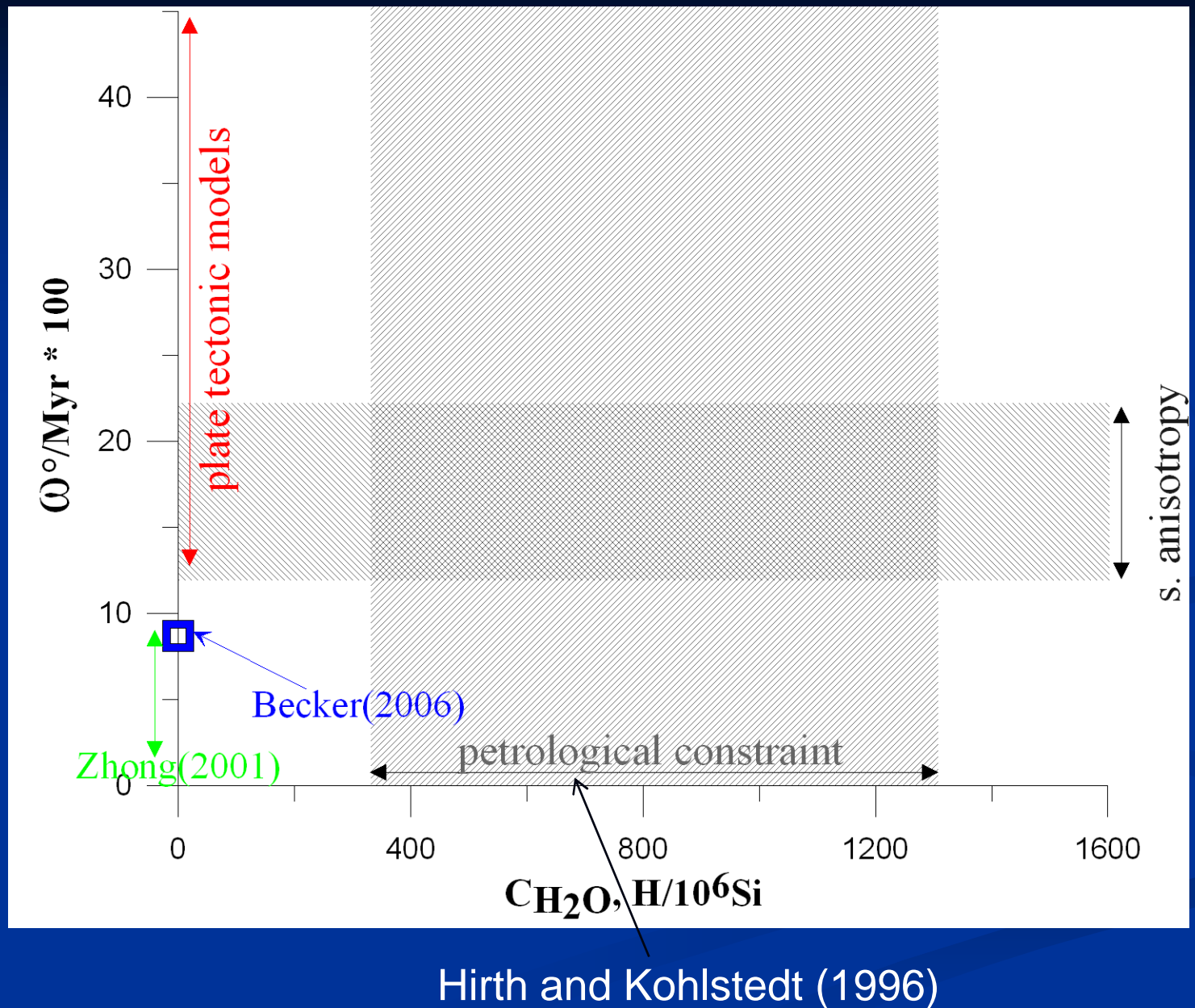
$$\mu_e = \mu \cdot (1 - P_{fl} / \sigma_n)$$

## Modeling scheme

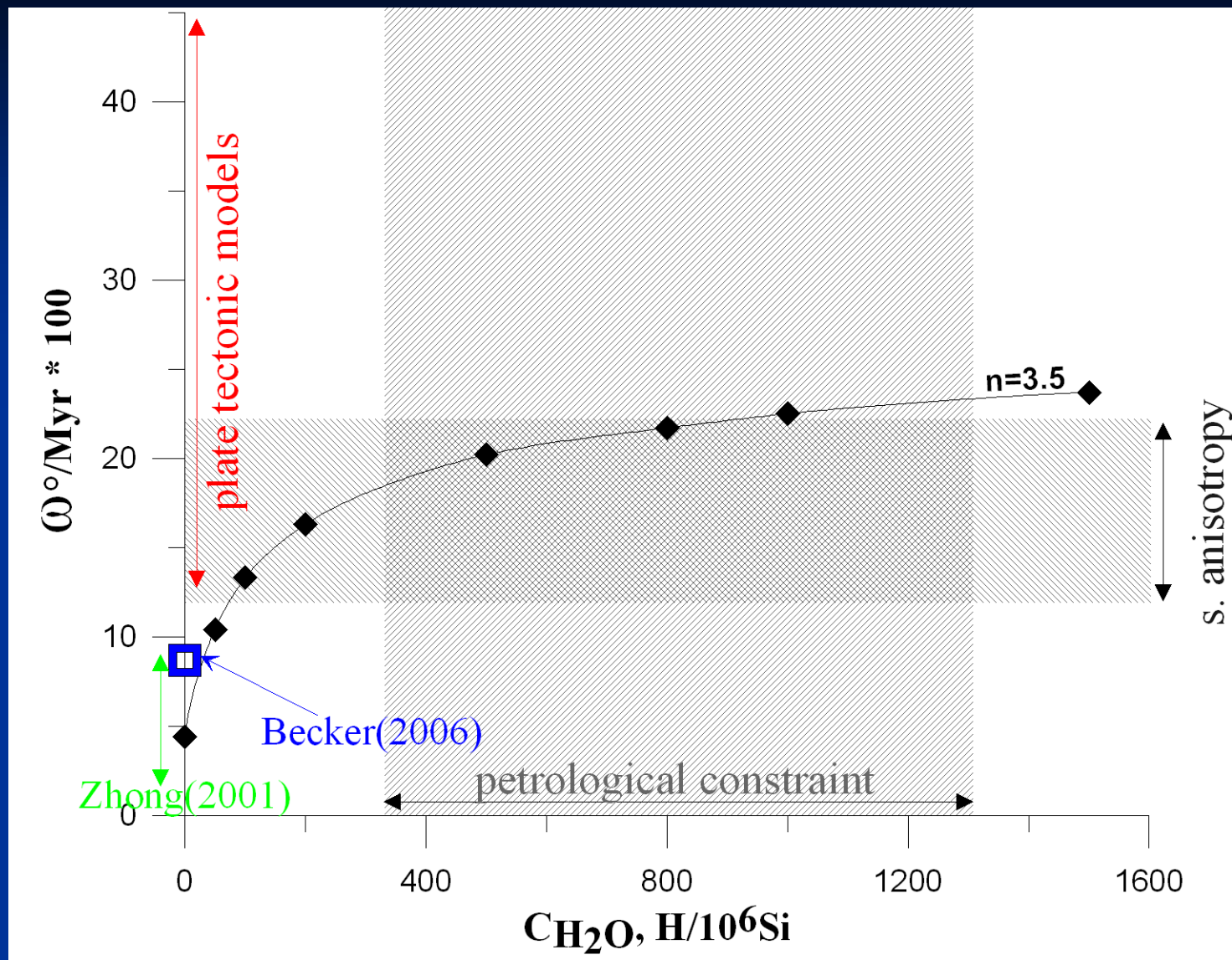
For every trial rheology (water content in asthenosphere) we calculate plate velocities for different frictions at plate boundaries, until we get best fit of observed plate velocities in the NNR reference frame

Next, we look how well those optimized models actually fit observations

# Lithospheric net rotation



# Lithospheric net rotation



# Lithospheric net rotation

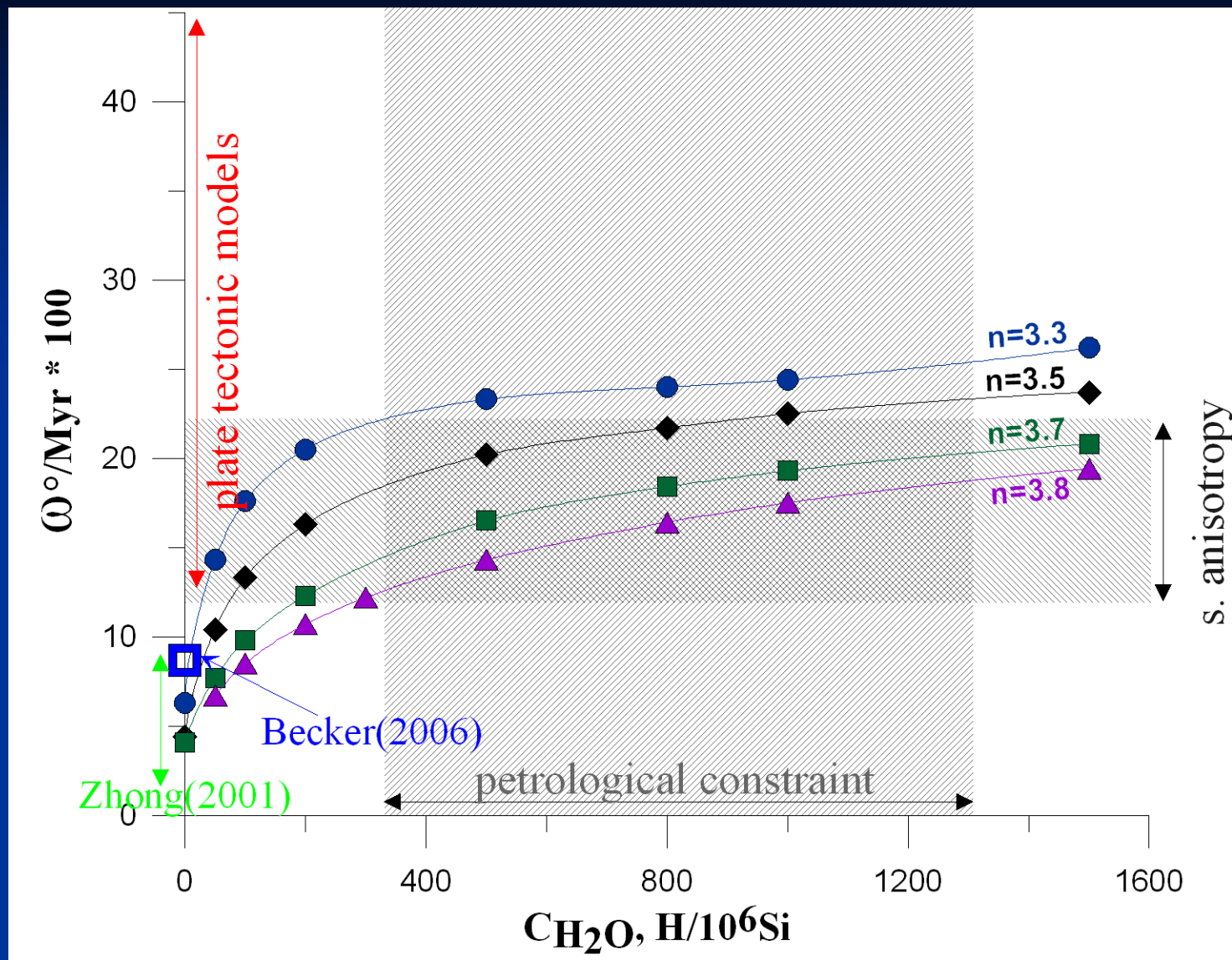
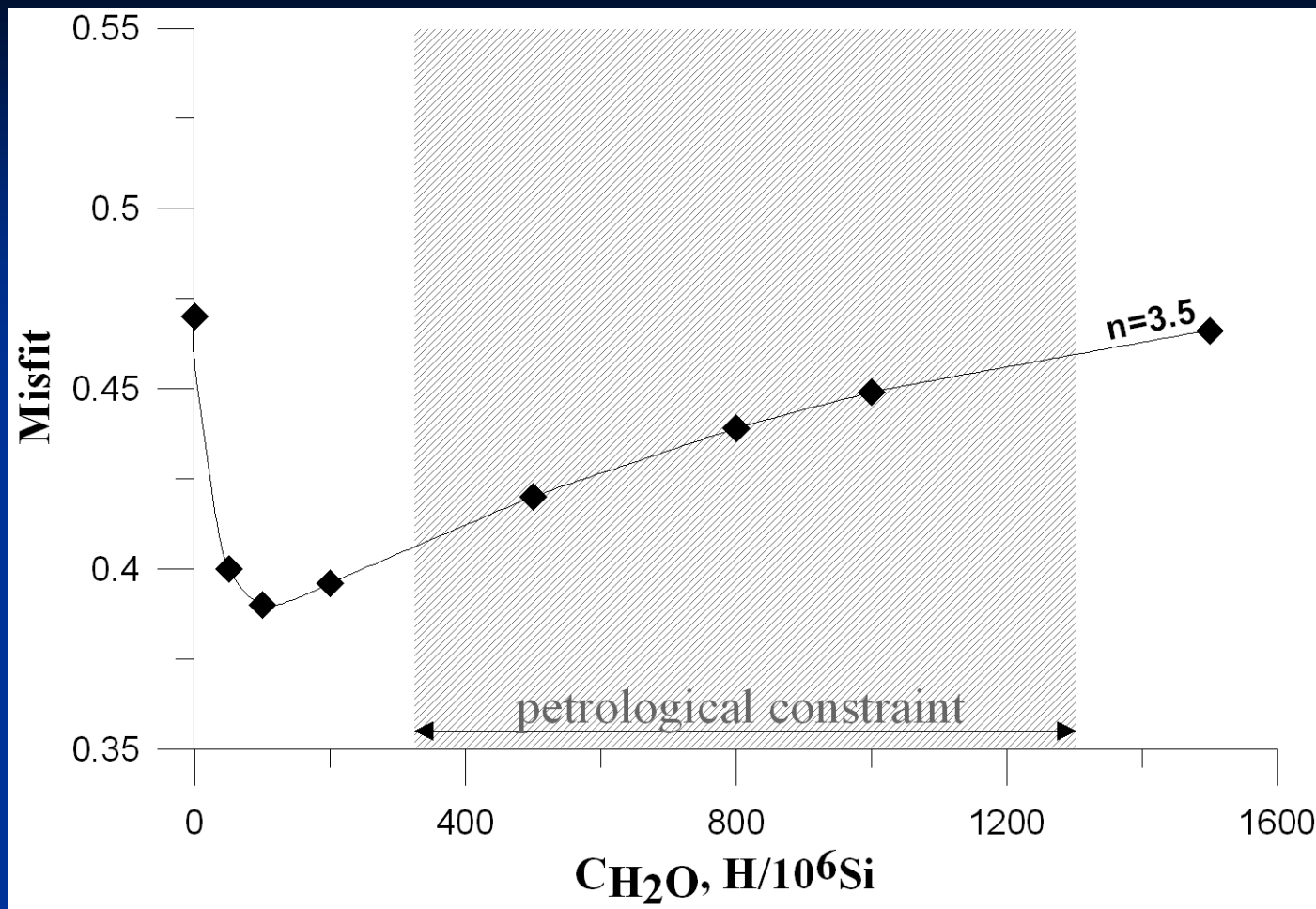
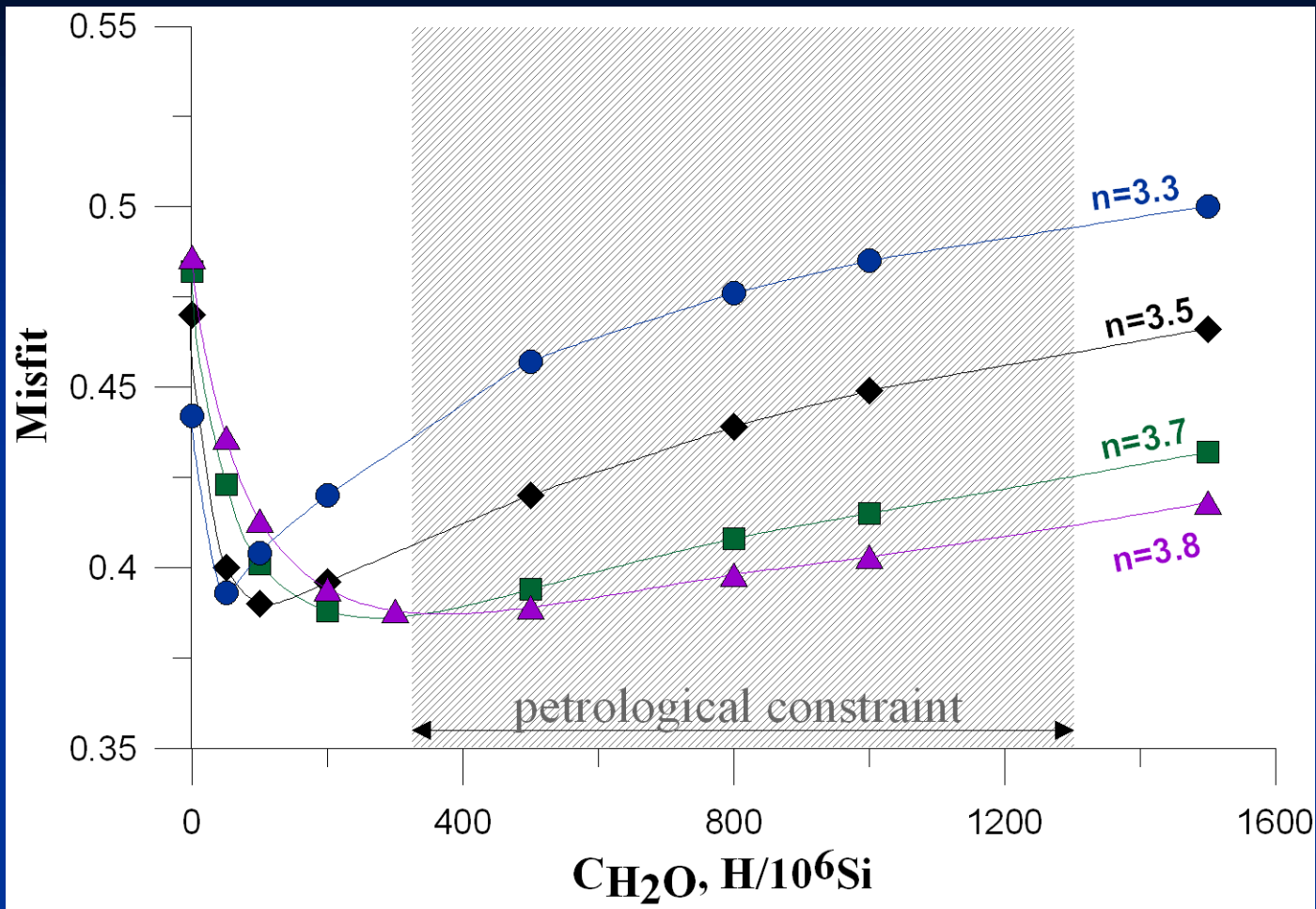


# Plate-velocities misfit



$$\text{Misfit} = \int \|\vec{v}_2 - \vec{v}_1\| / \|\vec{v}_1\| dS$$

# Plate-velocities misfit



$$\text{Misfit} = \int \|\vec{v}_2 - \vec{v}_1\| / \|\vec{v}_1\| dS$$

# Plate velocities in NNR reference frame Model

T<sub>p</sub>=1300°C,

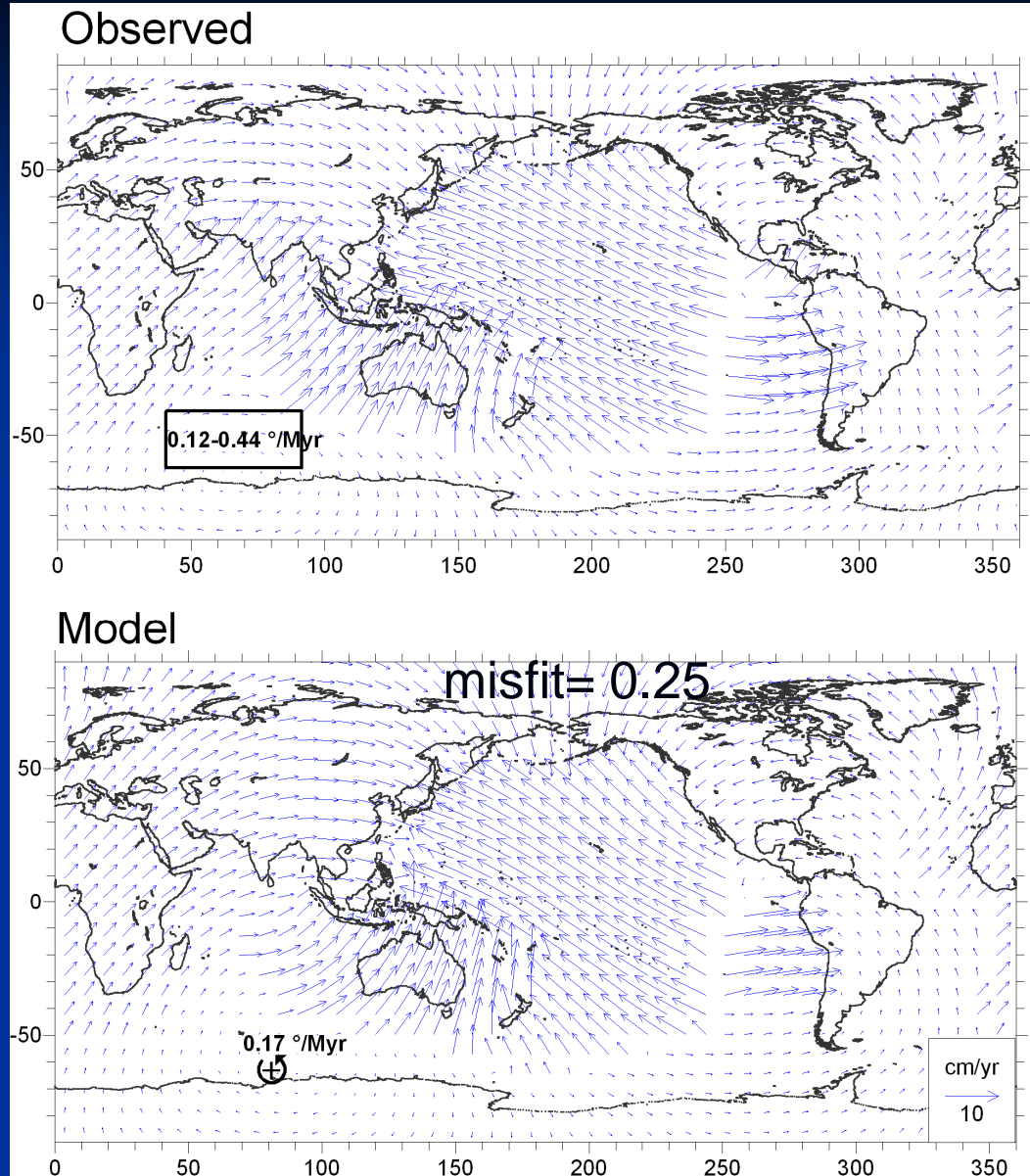
lith: dry olivine;

asth: 1000 ppm H/Si in  
olivine, n=3.8

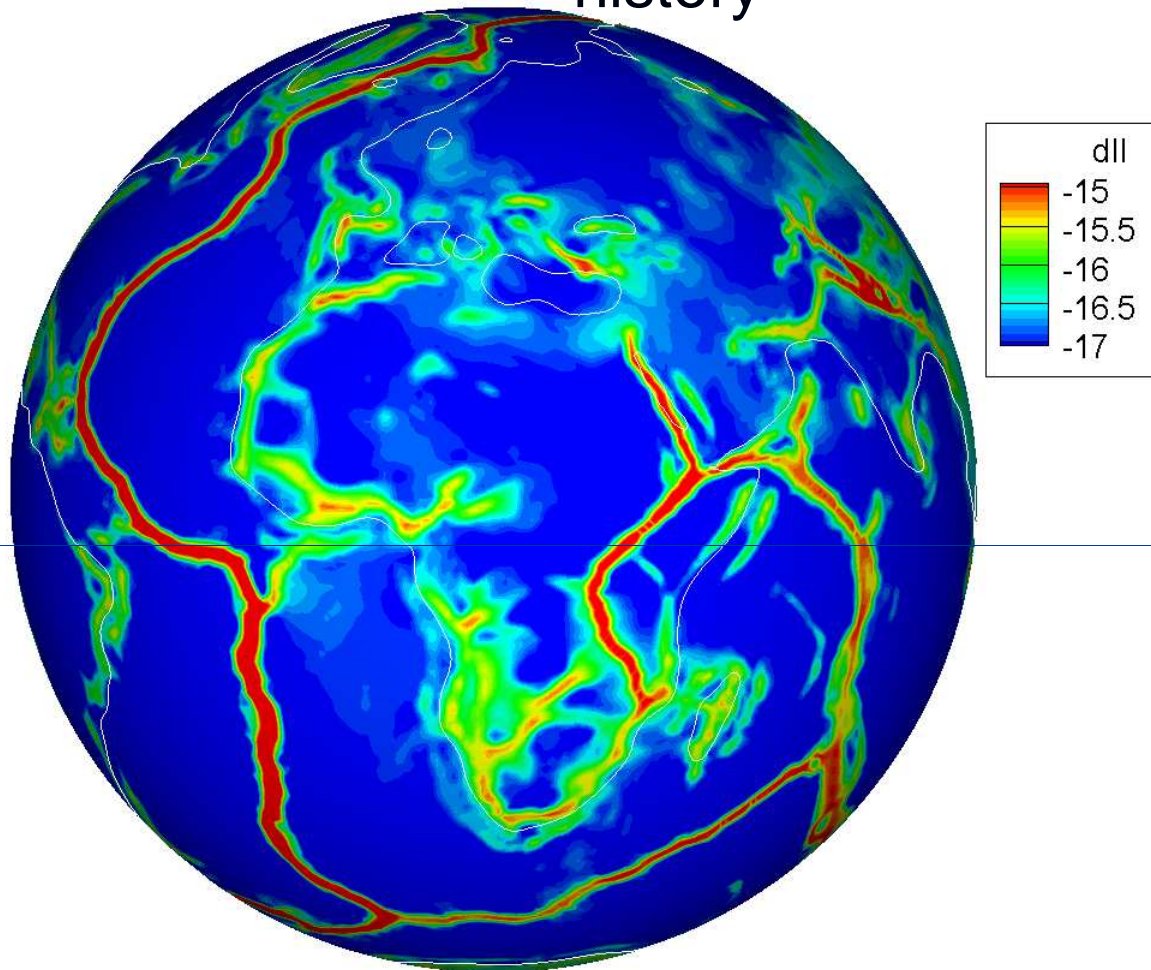
**Plate bound. friction:**

Subd. zones 0.01-0.03,  
other 0.05-0.15

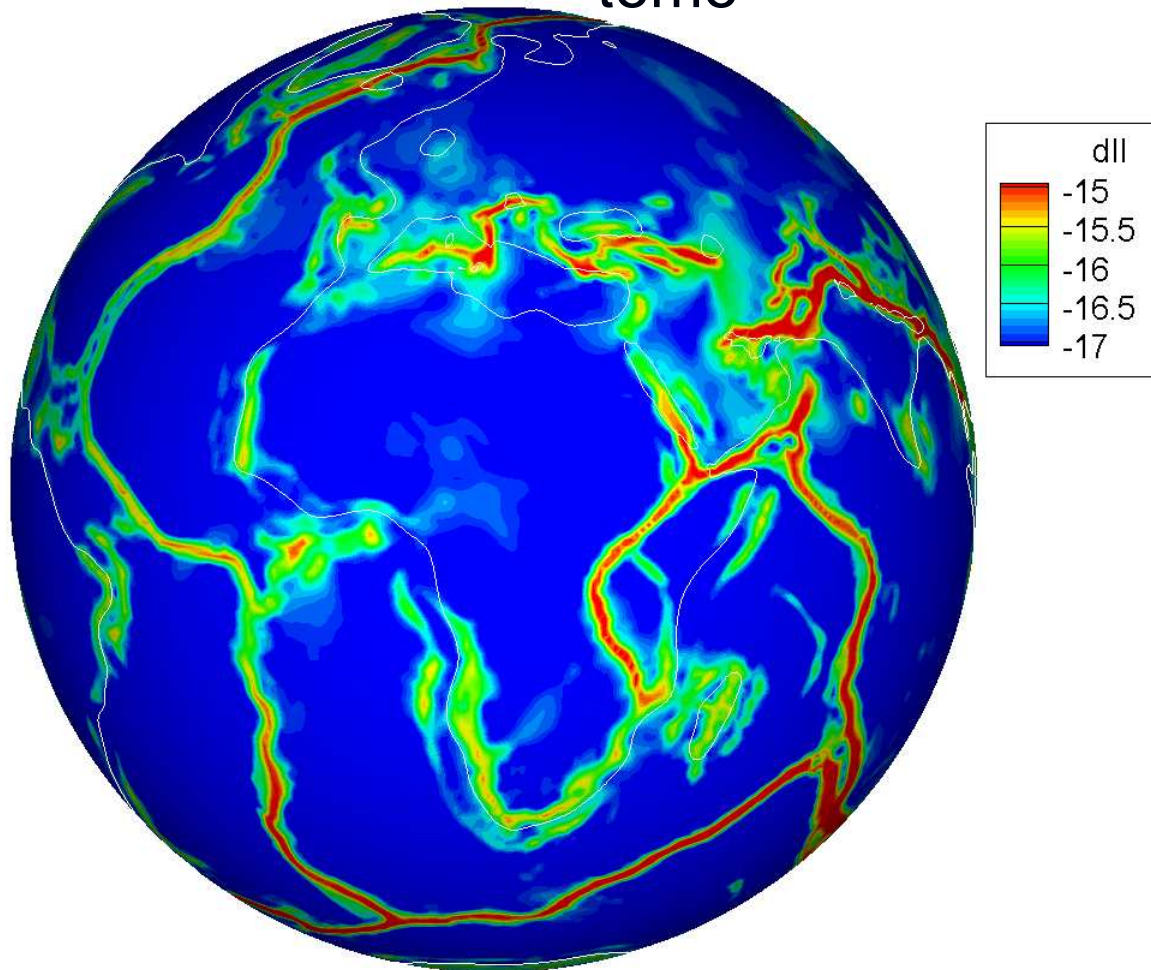
[misfit=0.25 \(0.36 previous  
best by Conrad and Lithgow-  
Bertelloni, 2004\)](#)



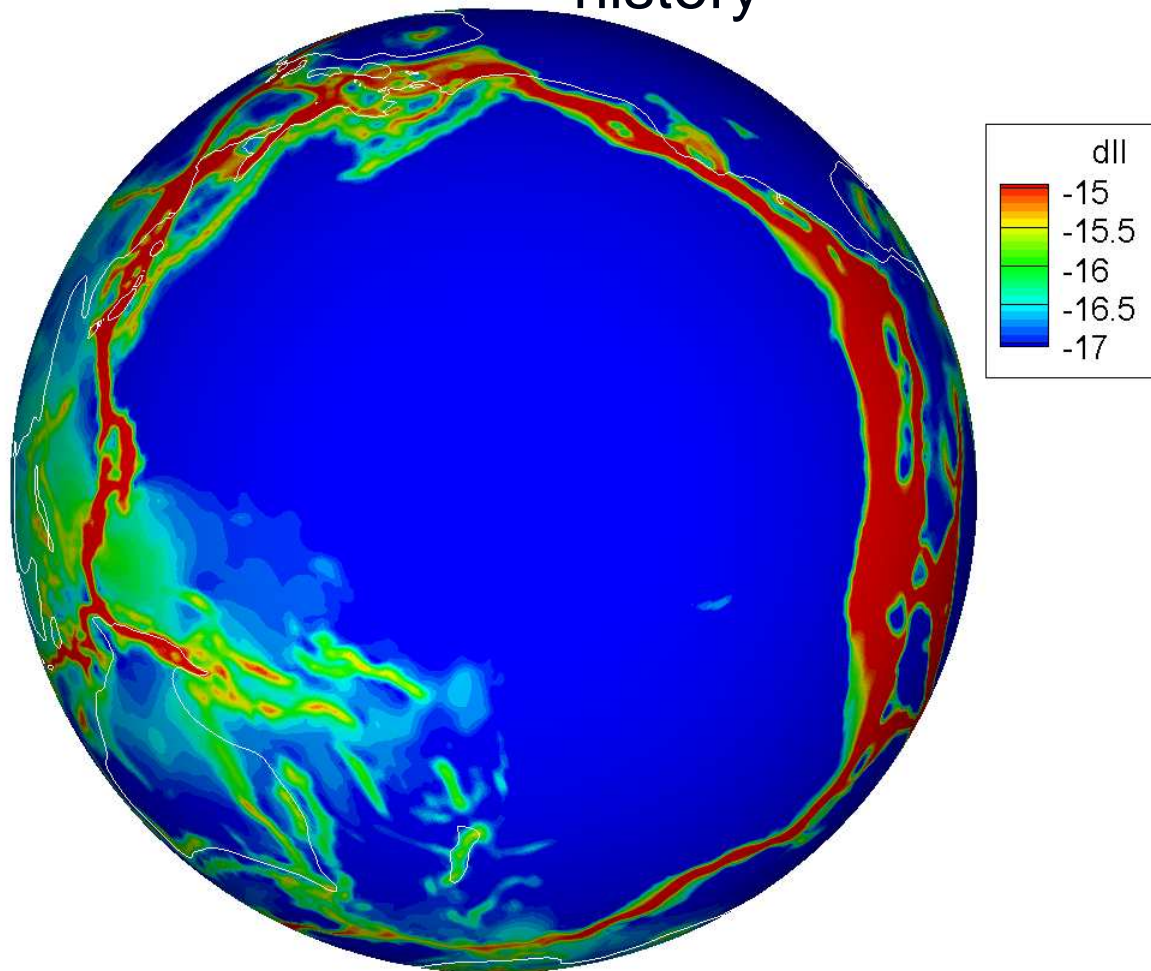
# Making plate boundaries: density distr. from subd. history



# Making plate boundaries: density distr. from smean tomo



# Making plate boundaries: density distr. from subd. history



# Conclusions

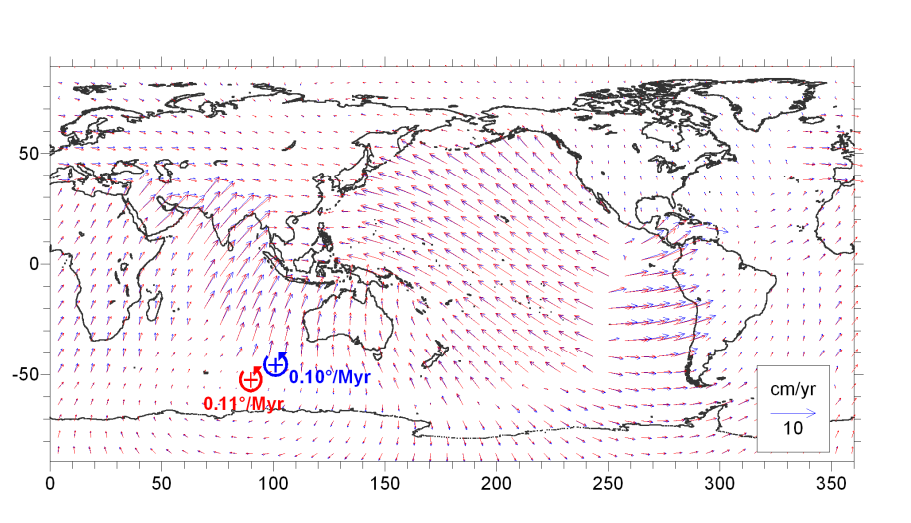
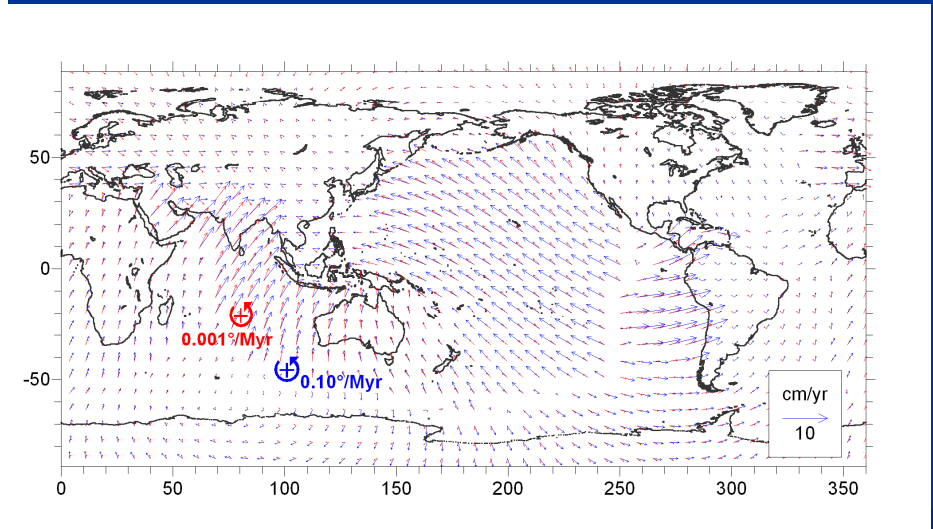
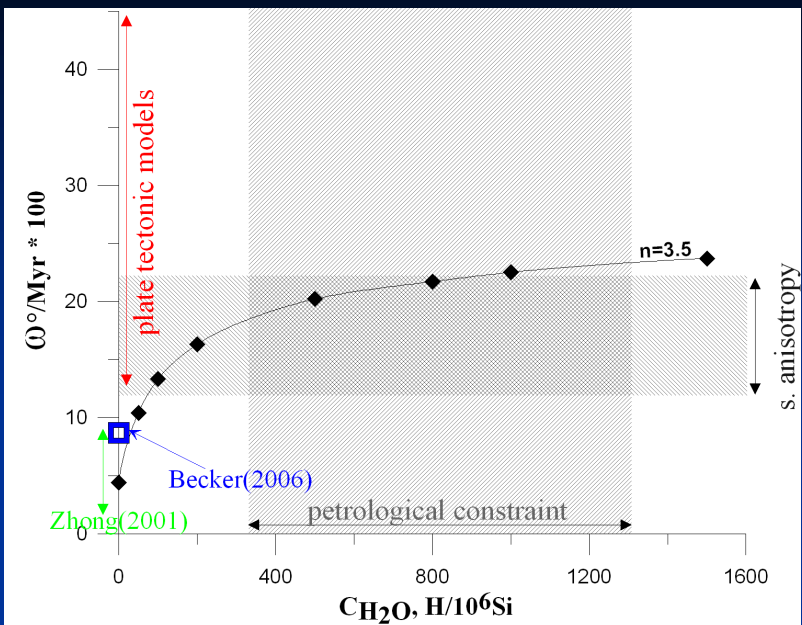


Plate velocities are not sensitive to the lateral viscosity variations deeper than 300 km

But their magnitudes are sensitive to the lateral viscosity variations shallower than 300 km

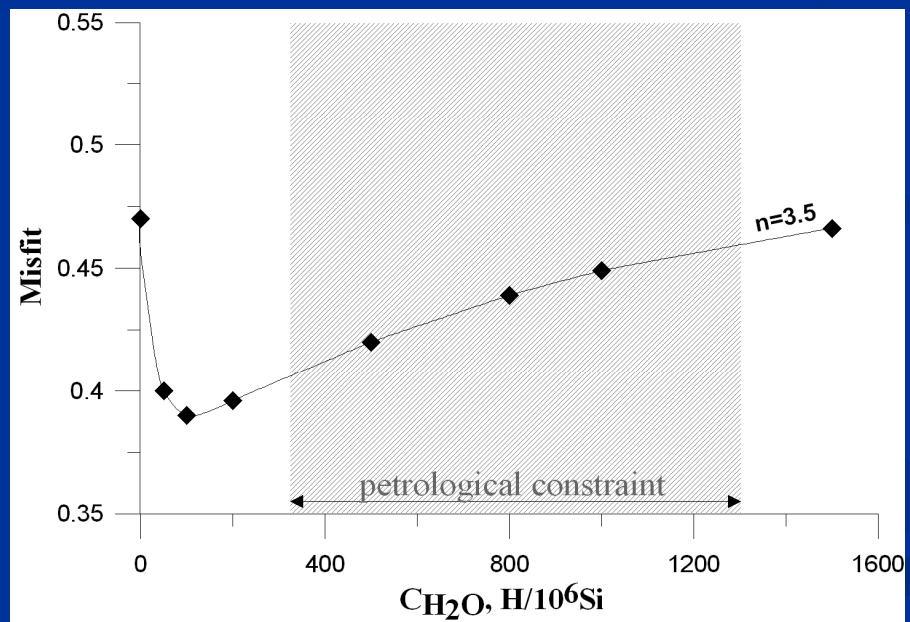


# Conclusions

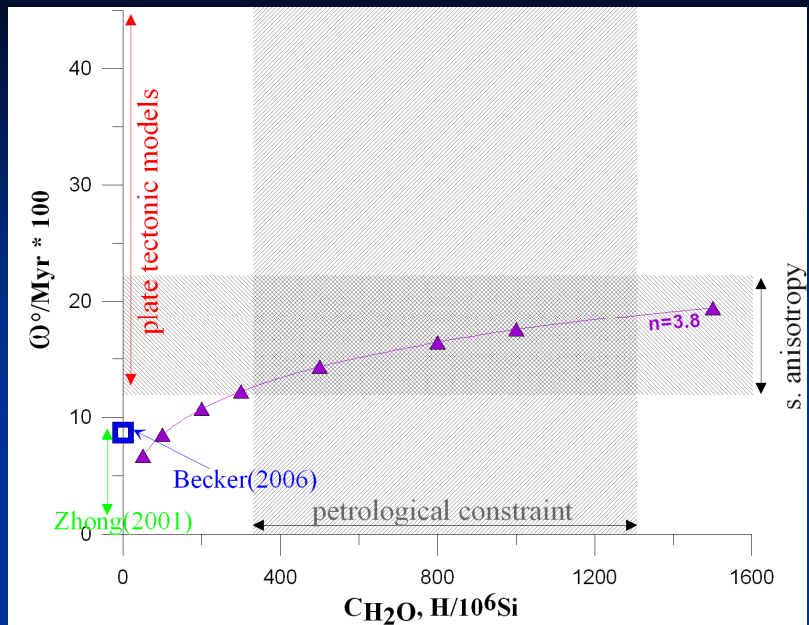


Magnitude of the lithospheric net rotation and quality of fit of plate velocities are sensitive to the water content of the asthenosphere

There is potential of estimating water content in the asthenosphere using plate velocities and net rotation

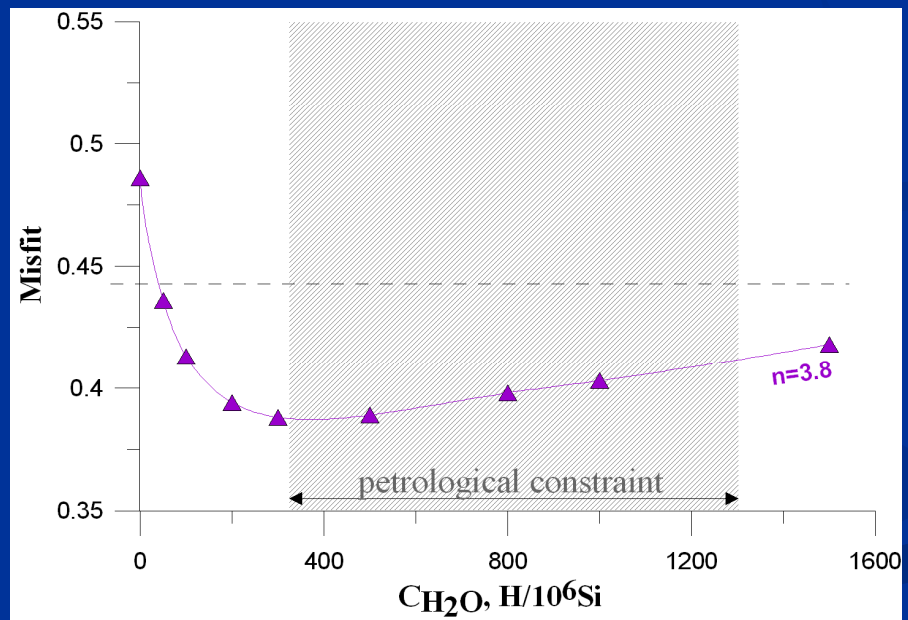


# Conclusions



if the stress exponent *in wet olivine rheology and activation volume* are pushed to the highest experimentally allowed values of  $n=3.8$ ,  $V=14$  cc/mol

The current views on the rheology and water content in the upper mantle are consistent with the observed plate velocities



# Conclusions

Distribution of dissipation rate

**No fluid = no plate tectonics**

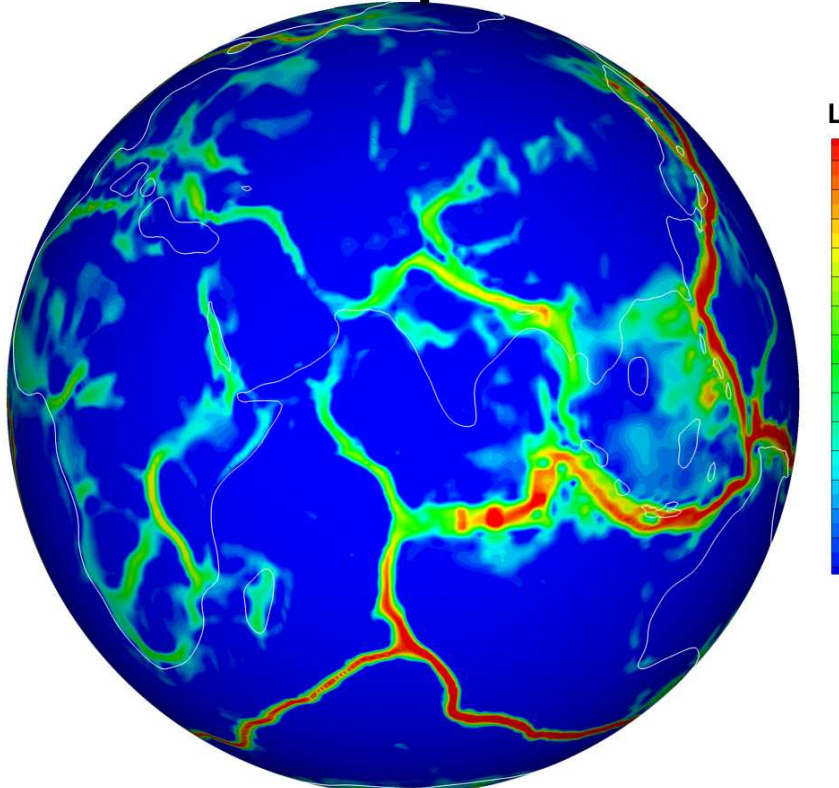


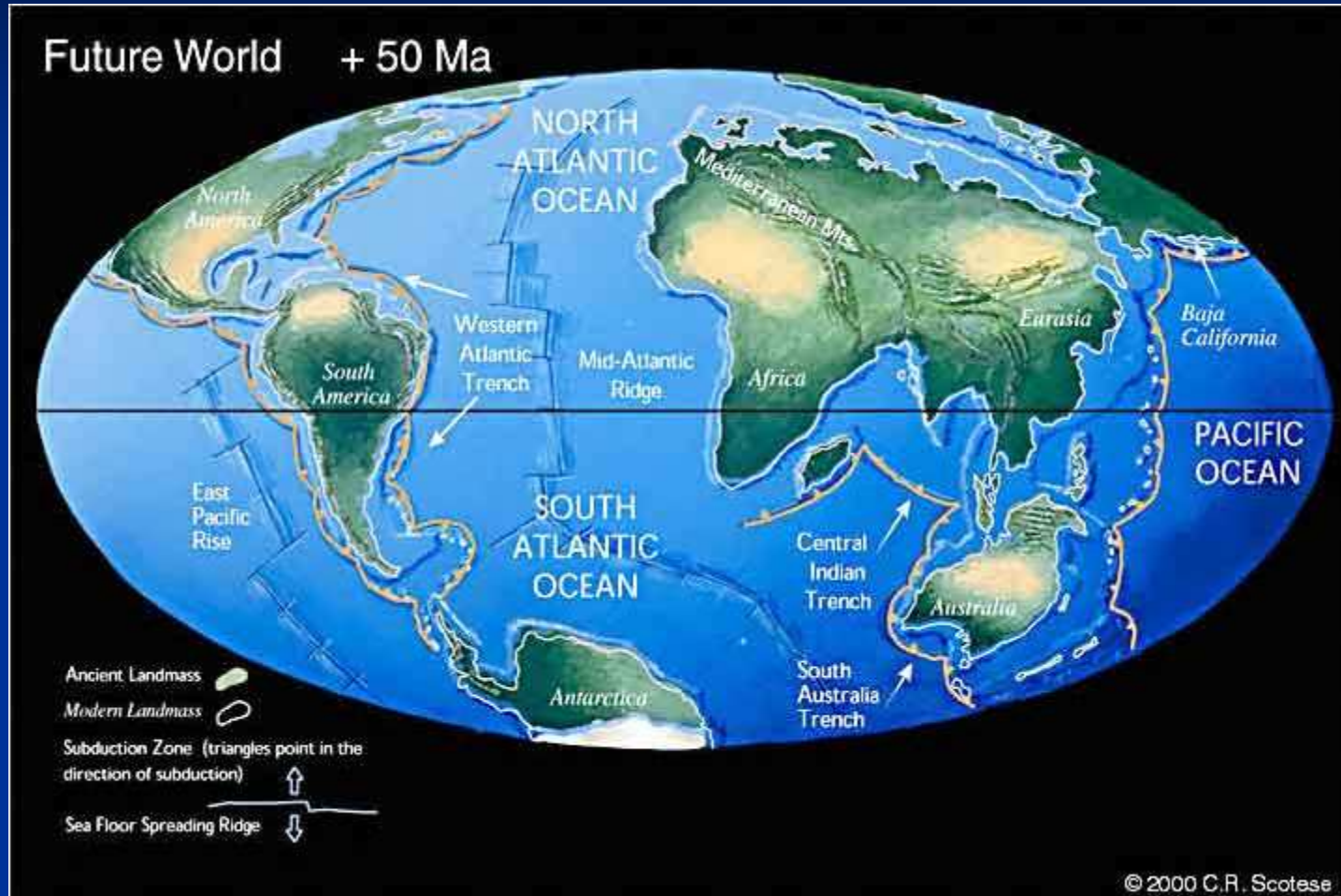
Plate boundaries must be very weak to allow for plate tectonics.

Particularly, at subduction zones friction must be < 0.02 on average, just some 1/35 of the dry rock value.

That can be achieved only with high-pressure fluids in subduction channels.

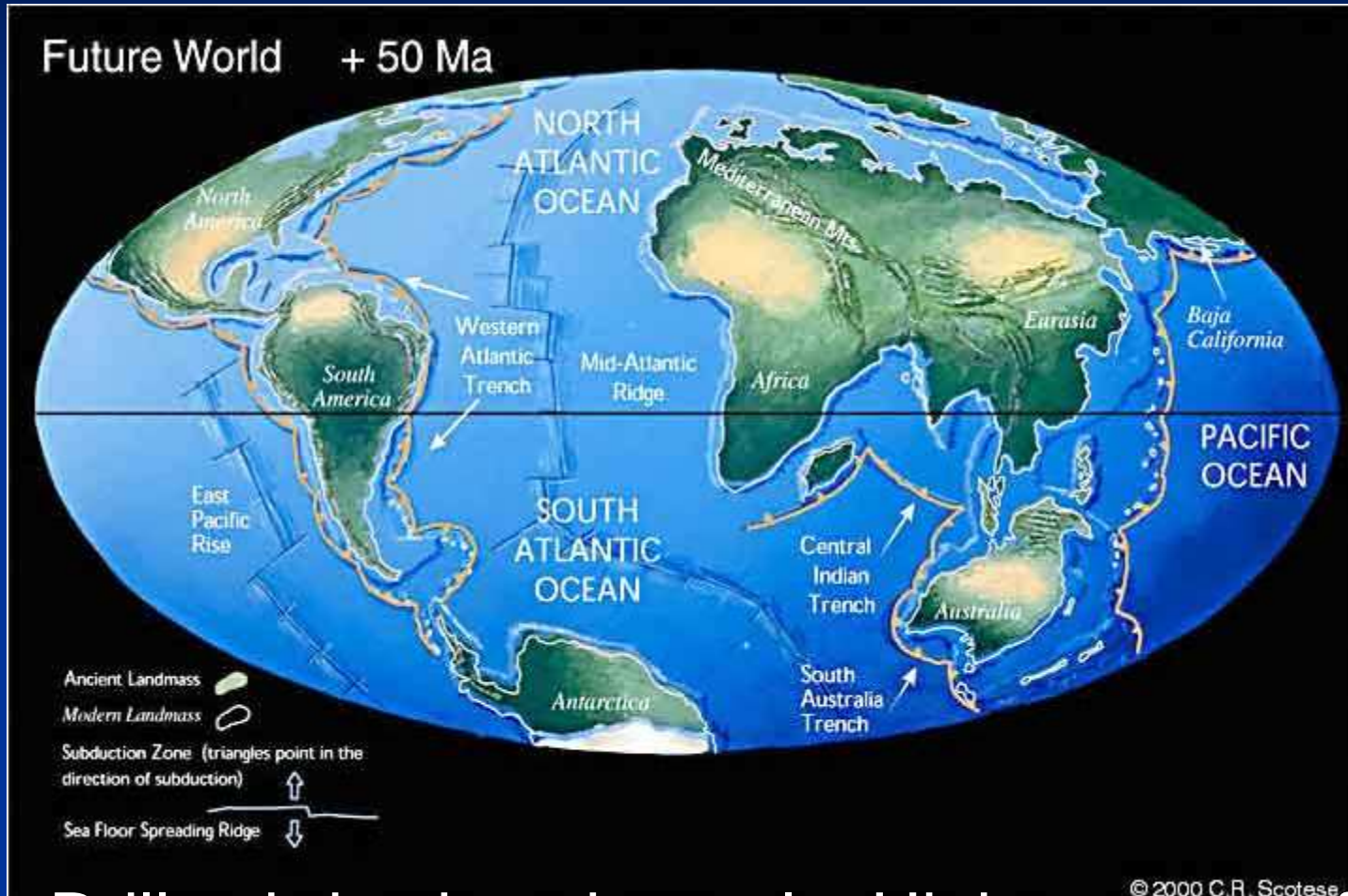
$$\mu_e = \mu \cdot (1 - P_{fl} / \sigma_n)$$

# Question for students



How to stop plate tectonics on the Earth?

# Question for students



Drill subduction channels. High-pressure fluid will come out and plate tectonics will stop